Metrologia 2014 **51** *Tech. Suppl.* 09006

Bilateral Comparison in Primary Angular Vibration Calibration

CCAUV.V-S1

Physikalisch-Technische Bundesanstalt PTB

Working Group 1.71 Acceleration

Angelika Täubner

Thomas Bruns

Abstract

A comparison CCAUV.V-S1 was organized to compare measurements of sinusoidal angular accelerations in the frequency range from 0.4 Hz to 1 kHz. This was a bilateral comparison between the Korea Research Institute of Standards and Science (KRISS), Republic of Korea, and the Physikalisch-Technische Bundesanstalt (PTB), Germany.

Both NMIs applied laser interferometry in compliance with ISO 16063-15:2006 “Methods for the calibration of vibration and shock transducers - Part 15: Primary angular vibration calibration by laser interferometry”.

The complex voltage sensitivity (magnitude and phase) of one angular transfer standard in the frequency range of 0.4 Hz to 100 Hz and the complex charge sensitivity (magnitude and phase) of one angular reference standard in the frequency range of 1 Hz to 1000 Hz were measured.

Table of Contents

1 INTRODUCTION

This report presents the results of the first bilateral CIPM comparison in the area of “angular vibration”. It has the status of a “Draft B”.

The Technical Protocol [5] specifies in detail the aim and the task of the comparison, the conditions of measurement, the angular acceleration standards used, measurement instructions and other items. A brief survey is given in the following sections.

This report summarizes the results obtained in the bilateral comparison CCAUV.V-S1 carried out between October 2012 and March 2013.

2 PARTICIPANTS

The following two laboratories were participants in the comparison of CCAUV.V-S1:

- Physikalisch-Technische Bundesanstalt (PTB), Germany, as pilot laboratory
- Korea Research Institute of Standards and Science (KRISS), Republic of Korea

3 TASK AND PURPOSE OF THE COMPARISON

According to the rules set up by the CIPM MRA, the consultative committees of the CIPM have the responsibility to establish “degrees of equivalence” (DoE) between the different measurement standards operated by the national NMIs. This is done by conducting key comparisons (KC) on different levels of the international metrological infrastructure. Specifically in the field of linear vibration, the first top level KC (CCAUV.V-K1) was finished in 2001 and the second KC (CCAUV.V-K2) was finished in 2014. Their results are the foundation of all subsequently established DoE in the field of linear vibration.

Unlike the field of linear vibration, however, neither bilateral comparisons nor KCs in the field of angular vibration have been done between NMIs. It is necessary that at least two NMIs, which have the capability of primary angular vibration calibration by laser interferometry, launch the first bilateral comparison.

The specific task of this comparison was to measure the complex charge (or voltage) sensitivity of two different angular accelerometers at specified frequencies with primary means, i.e. according to ISO 16063-15 “Methods for the calibration of vibration and shock transducers - Part 15: Primary angular vibration calibration by laser interferometry”.

The reported sensitivities and associated uncertainties are used for the calculation of the DoE between the participating NMIs and the comparison reference values.

4 MEASUREMENT CONDITIONS

For the calibration task of this bilateral comparison, two angular accelerometers, working standards of PTB and KRISS, were circulated between two laboratories. The two angular accelerometer working standards are presented in Section 5. The measurement conditions are given in following.

The angular accelerometers were supposed to be calibrated for the magnitude and the phase of their complex charge and voltage sensitivity according to those procedures and conditions implemented by the NMI in conformance with ISO 16063-15. The charge/voltage sensitivities should be reported for the accelerometers alone. The measurement frequency range was chosen from 0.4 Hz to 1 kHz. Specifically, the laboratories were supposed to measure at the following frequencies (all values in Hz): 0.4, 0.5, 0.63 (or 0.64), 0.8, 1, 1.25, 1.6, 2, 2.5, 3.15 (or 3.2), 4, 5, 6.3 (or 6.4), 8, 10, 12.5, 16, 20, 25, 31.5 (or 32), 40, 125, 160, 200, 250, 315 (or 320), 400, 500, 630 (or 640), 800, and 1000.

The participating laboratories should provide magnitude and phase results over the whole frequency range supported by their system.

The charge amplifier used for the calibration was not provided with the set of artefacts, but had to be provided by each participant.

The measurement conditions should be kept according to the laboratory's standard conditions for calibration of customer accelerometers for claiming their best measurement capability or CMCs where applicable. This presumes that these conditions comply with those defined by the applicable ISO documentary standards [1, 2, 3].

Actual measurement conditions during this comparison may depend on the primary angular vibration systems at KRISS and PTB. The following recommended conditions and the ones actually measured should be reported by the participants:

- The applied acceleration levels at the measured frequencies should be reported as Peak angular acceleration amplitudes in rad/s^2.
- Ambient temperature and accelerometer temperature during the calibration: (23 ± 2) °C, with actually measured values to be stated within tolerances of ± 0.3 °C.
- Relative humidity max.: 75 %.
- Mounting torque of the accelerometer: (2.0 ± 0.1) N·m.

5 ANGULAR ACCELERATION STANDARDS

The two artefacts circulated in this comparison were the following angular accelerometers working standards:

- PTB working standard “single-ended” being a servo angular accelerometer Jewell, type ASMP-200, SN 50563.
- KRISS working standard “back-to-back” being a piezoelectric angular accelerometer Brüel&Kjaer (B&K), type 4381-ROT, SN 30001.

In the following, both angular accelerometers under calibration will be abbreviated as Jewell ASMP-200 and B&K 4381-ROT.

For the purpose of monitoring the temporal stability of the accelerometer Jewell ASMP-200, the pilot laboratory has monitored its sensitivity for about five years prior to the start of the comparison measurements.

The Korea Research Institute of Standards and Science (KRISS) has monitored the B&K4381-ROT for about three years prior to the start of the comparison measurements. The investigation of the long-term stability was continued throughout the circulation period. The results of the PTB and KRISS stability measurements and other individual data of the angular standards are given in Section 7.

The results obtained by the PTB for the working standard Jewell ASMP-200 were reported to the BIPM in October 2012, before having access to any of the results reported by KRISS. The purpose of this was to have the BIPM as a witness of the pilot laboratory results before any exchange of measurement results between the participants.

These previous monitoring “results reported to BIPM” by the PTB were still without consideration of the output impedance of this accelerometer and the input impedance of the voltage measurement system.

During the evaluation of the measurement results of PTB and KRISS of the angular accelerometer Jewell ASMP-200, it was found that the output impedance of this accelerometer and the input impedance of the voltage measuring system used had to be considered in terms of a systematic correction for the magnitude of the complex voltage sensitivity (see Section 7.3.1).

6 CIRCULATION OF THE ANGULAR ACCELERATION STANDARDS

The two angular accelerometers were circulated during the measurement period of four weeks provided for each participant. The initial and final measurements were made by the pilot lab in order to monitor the stability and any change of the vibration response characteristics of the artefacts. The measurement and monitoring dates for both angular accelerometers were as follows:

Measurement and monitoring dates of the PTB working standard angular accelerometer Jewell ASMP-200

Participant	Measurement Month	Shipping	Monitoring
PTB	09/2012	12/2012	10/2012
KRISS	01/2013	02/2013	02/2013
PTB	03/2013		

Measurement and monitoring dates of the KRISS working standard angular accelerometer B&K 4381-ROT

Participant	Measurement Month	Shipping	Monitoring
KRISS	10/2012	12/2012	02/2013
PTB	01/2013	02/2013	03/2013

7 RESULTS OF MEASUREMENTS

7.1 Long-term stability

For the purpose of monitoring the long-term stability of the Jewell ASMP-200, the pilot laboratory (PTB) had monitored its complex voltage sensitivity in the frequency range 0.4 Hz to 100 Hz for about 5 years prior to the start of the comparison measurements. At all frequencies, magnitude and phase shift measurements were carried out from 2008 to 2012. These measurements were used to evaluate the relative standard deviation and the expanded measurement uncertainty given in Table 1. Figure 1 shows the magnitude $S_{u\alpha}$ of the complex voltage sensitivity $\underline{S}_{u\alpha}$ measured at the reference frequency of 16 Hz during the monitoring period of five years.

KRISS had monitored the complex charge sensitivity of the B&K 4381-ROT in the frequency range of 1 Hz to 1000 Hz for about 3 years prior to the start of the comparison measurements. The investigation of the long-term stability was continued throughout the circulation period. Table 2 shows the standard deviation and the expanded uncertainty of the magnitude and phase shift of the angular accelerometer B&K 4381-ROT, measured from 2011 to 2013. Figure 2 shows the magnitude $S_{q\alpha}$ of the complex charge sensitivity $\underline{S}_{q\alpha}$ measured at 16 Hz during three years.

Any noticeable change of the complex sensitivity of the two circulated angular accelerometers was not found in the long-term stability monitored by both participants before and during this comparison.

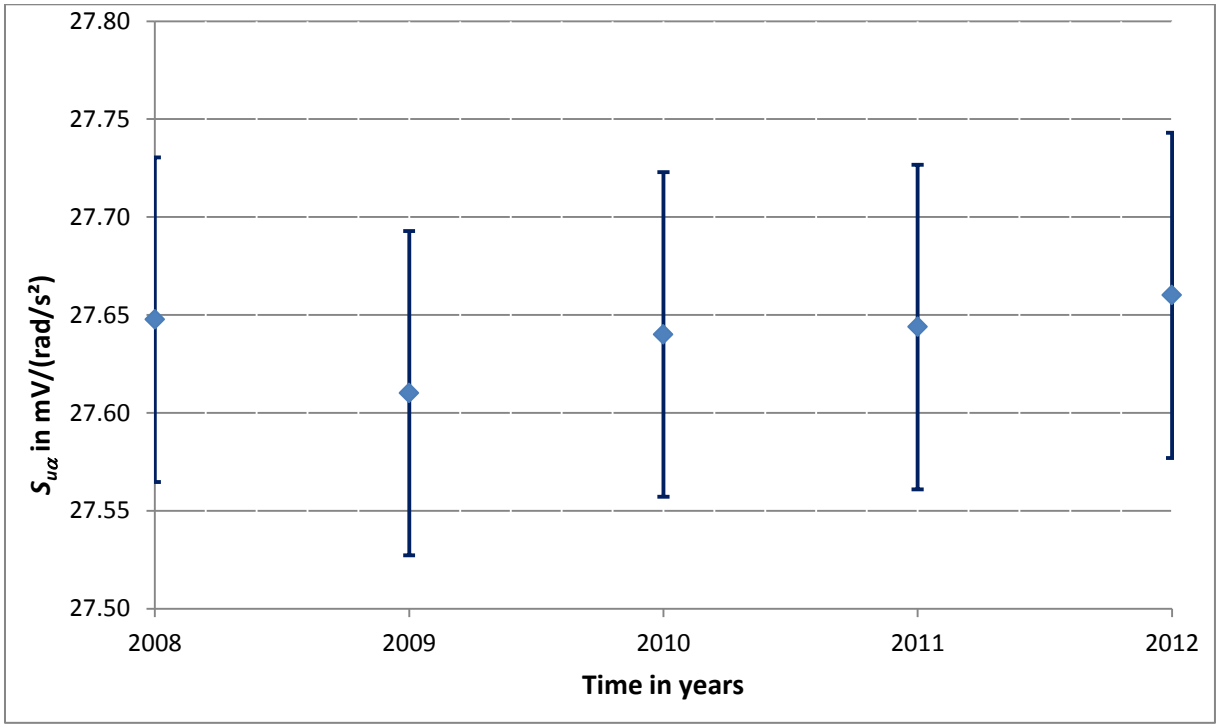

Figure 1: Long-term stability of the magnitude $S_{u\alpha}$ of the complex voltage sensitivity $\underline{S}_{u\alpha}$ of the Jewell ASMP-200 of five series of measurement during five years at the reference frequency of 16 Hz. The error bars represent 0.3 % expanded measurement uncertainty (k = 2).

Table 1: Standard deviation of the complex voltage sensitivity of the Jewell ASMP-200 during five years from 2008 to 2012, measured at PTB in the frequency range of 0.4 Hz to 100 Hz.

Frequency in Hz	Angular Acceleration in rad/s²	Rel. Standard Deviation Magnitude in %	Expanded Uncertainty in %	Standard Deviation Phase Shift in °	Expanded Uncertainty in °
0.4	1	0.04	0.3	-0.11	0.5
0.5	2	0.04	0.3	-0.09	0.5
0.64	4	0.04	0.3	-0.10	0.5
0.8	7	0.03	0.3	-0.01	0.5
1	11	0.03	0.3	-0.10	0.5
1.25	11	0.04	0.3	-0.06	0.5
1.6	12	0.04	0.3	-0.03	0.5
2	15	0.03	0.3	-0.02	0.5
2.5	16	0.03	0.3	-0.03	0.5
3.2	13	0.04	0.3	-0.01	0.5
4	13	0.04	0.3	-0.03	0.5
5	13	0.02	0.3	0.00	0.5
6.4	14	0.02	0.3	0.00	0.5
8	15	0.02	0.3	-0.01	0.5
10	17	0.03	0.3	0.00	0.5
12.5	20	0.04	0.3	-0.01	0.5
16	24	0.03	0.3	-0.01	0.5
20	28	0.03	0.3	-0.01	0.5
25	34	0.03	0.3	-0.01	0.5
32	41	0.04	0.3	-0.01	0.5
40	50	0.03	0.3	-0.01	0.5
50	56	0.05	0.3	-0.01	0.5
64	64	0.17	0.6	-0.01	0.5
80	64	0.32	0.6	0.00	0.5
100	95	0.13	0.6	0.00	0.5

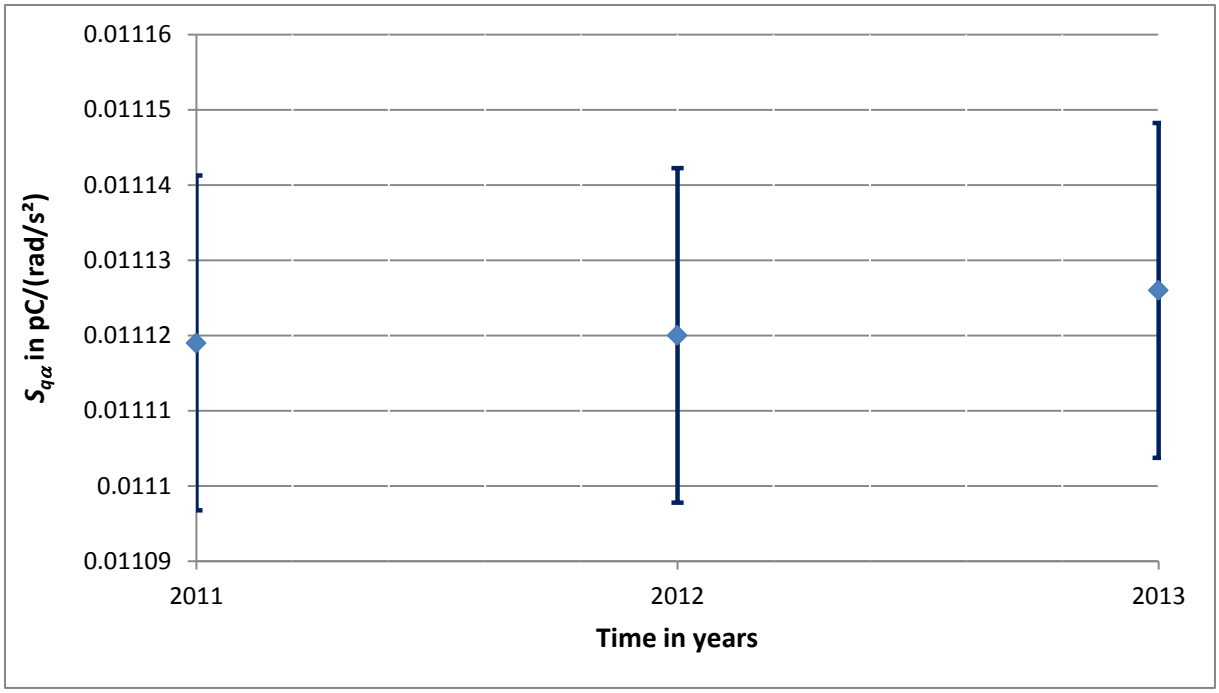

Figure 2: Long-term stability of the magnitude $S_{q\alpha}$ of the complex charge sensitivity $\underline{S}_{q\alpha}$ of the B&K 4381-ROT during three years at the reference frequency of 16 Hz. The error bars represent 0.2 % expanded measurement uncertainty (k = 2).

Table 2: Standard deviation of the complex charge sensitivity of the B&K 4381-ROT during three years, measured at KRISS in the frequency range of 1 Hz to 1000 Hz.

Frequency in Hz	Angular Acceleration in rad/s²	Rel. Standard Deviation Magnitude in %	Expanded Uncertainty in %	Standard Deviation Phase Shift in ° x 10^{-2}	Expanded Uncertainty in °
1	10	0.087	0.5	2.07	0.2
1.25	14.1	0.087	0.5	2.07	0.2
1.6	25	0.087	0.3	2.07	0.1
2	40	0.087	0.3	2.07	0.1
2.5	50	0.078	0.2	2.07	0.1
3.2	70.7	0.070	0.2	2.07	0.1
4	100	0.060	0.2	2.07	0.1
5	100	0.060	0.2	2.07	0.1
6.4	100	0.059	0.2	2.07	0.1
8	141.4	0.059	0.2	2.07	0.1
10	141.4	0.059	0.2	2.07	0.1
12.5	141.4	0.057	0.2	0.68	0.1
16	141.4	0.054	0.2	0.68	0.1
20	141.4	0.052	0.2	0.68	0.1
25	141.4	0.050	0.2	0.68	0.1
32	141.4	0.050	0.2	0.68	0.1
40	141.4	0.050	0.2	0.68	0.1
50	141.4	0.050	0.2	0.68	0.1
64	141.4	0.050	0.2	0.68	0.1
80	141.4	0.050	0.2	0.68	0.1
100	141.4	0.050	0.2	0.68	0.1
125	141.4	0.050	0.2	0.68	0.1
160	141.4	0.050	0.2	0.68	0.1
200	282.4	0.050	0.2	0.68	0.1
250	282.4	0.050	0.2	0.68	0.1
320	282.4	0.050	0.2	1.00	0.1
400	282.4	0.050	0.3	1.00	0.2
500	282.4	0.050	0.4	4.64	0.3
640	565.7	0.137	0.5	4.64	0.3
800	565.7	0.262	0.7	5.38	0.3
1000	565.7	0.589	1.3	65.47	1.4

In addition to the technical protocol, the calibration results (i.e. frequency responses of the complex voltage sensitivity $\underline{S}_{u\alpha}$, see Section 7.3) of the Jewell ASMP-200 measured at the end of the circulation period (March 2013) at PTB were compared with the previous monitoring results obtained in October 2012 and reported to BIPM. This comparison is shown in Figures 3 and 4.

a)

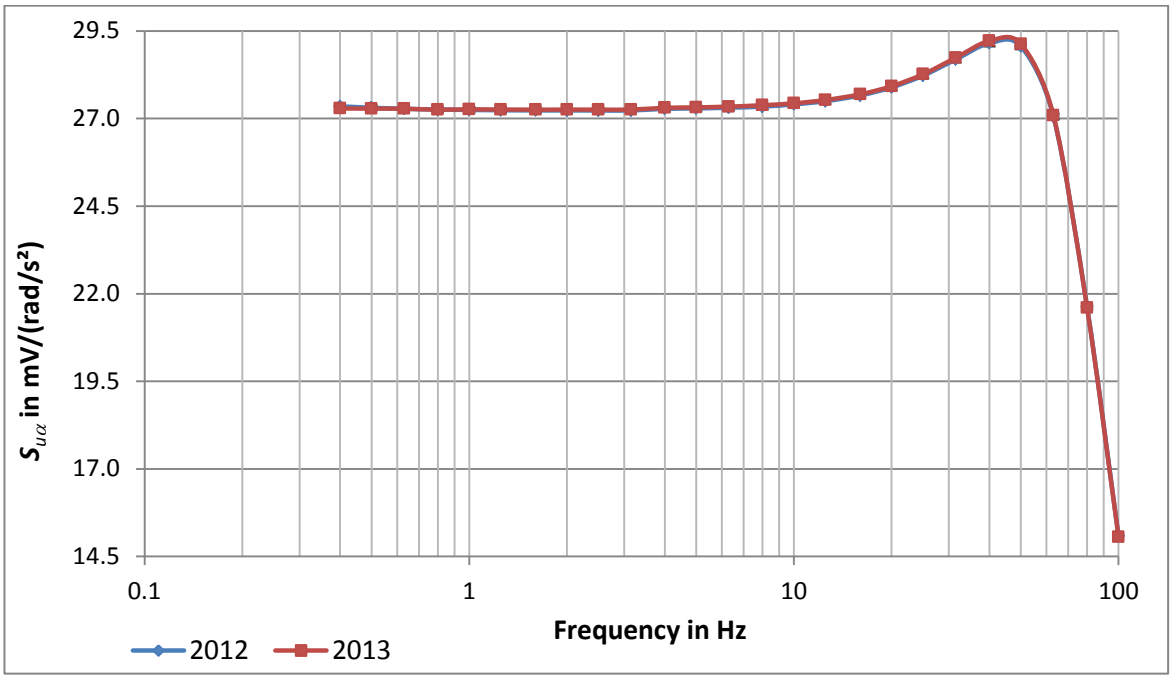

b)

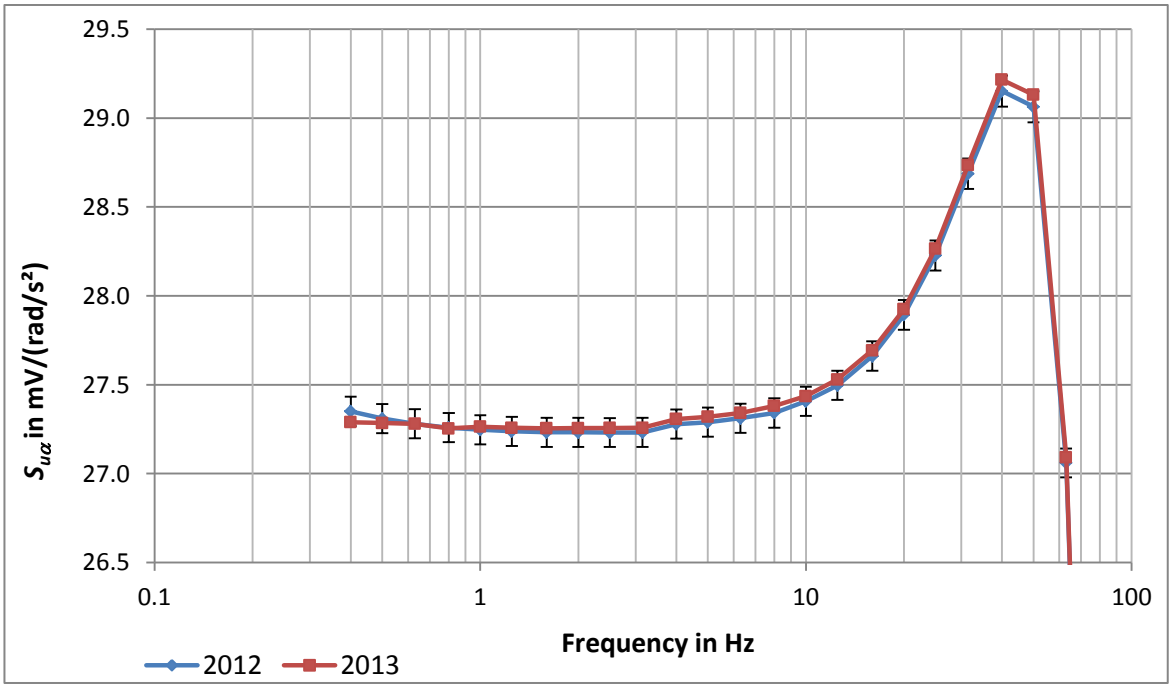

Figure 3: Magnitude $S_{u\alpha}$ of the complex voltage sensitivity $\underline{S}_{u\alpha}$ of the Jewell ASMP-200 in the frequency range of 0.4 Hz to 100 Hz (values measured at PTB in 2012, as reported to BIPM, and in March 2013 after being returned from KRISS). The 2012 data is plotted with error bars representing the expanded measurement uncertainty (k = 2). The values are without the correction of the influence of the impedance.

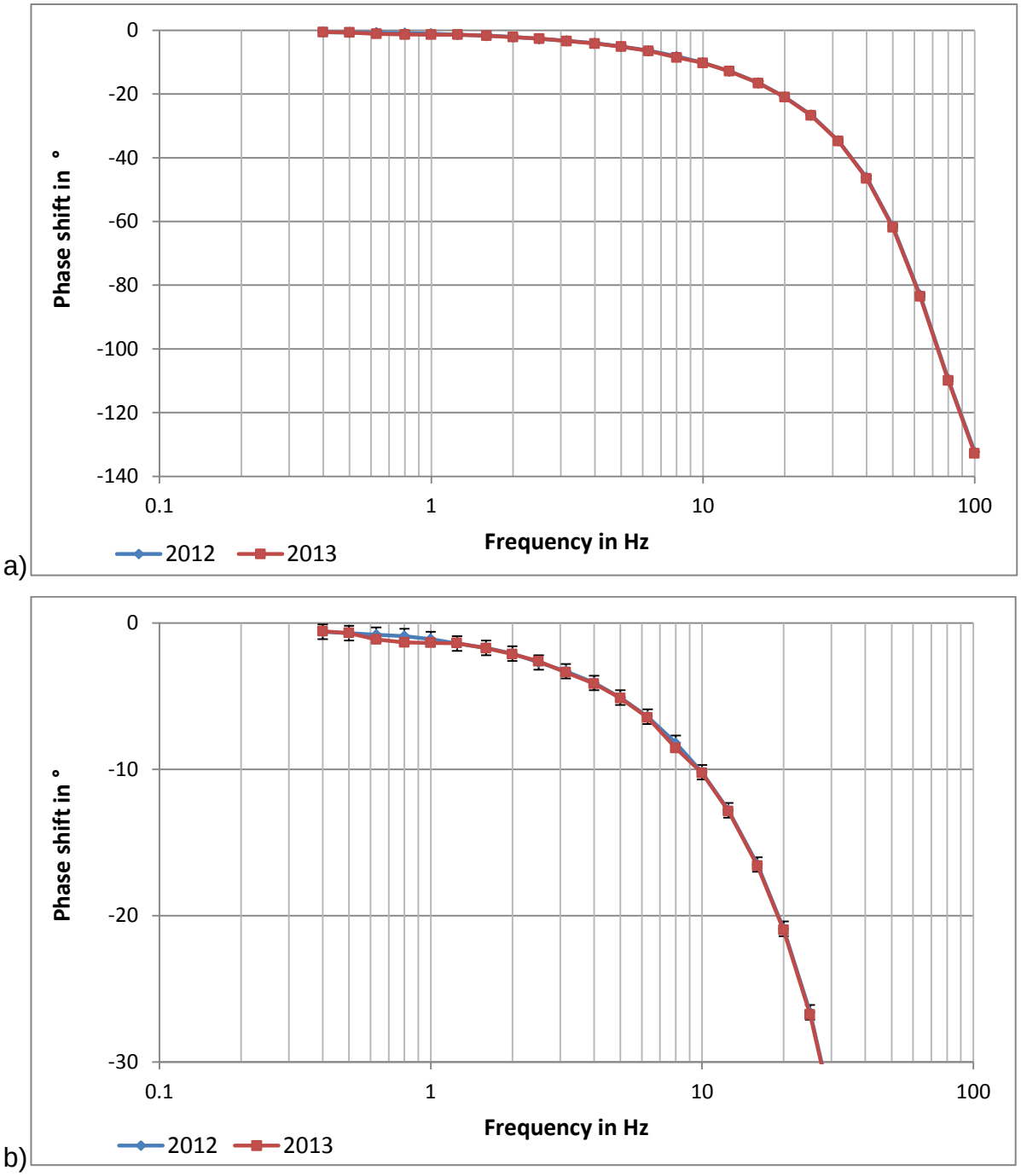

Figure 4: Phase shift $\Delta\varphi_{u\alpha}$ of the complex voltage sensitivity $\underline{S}_{u\alpha}$ of the Jewell ASMP-200 in the frequency range of 0.4 Hz to 100 Hz (values measured at PTB in 2012 and in March 2013 after being returned from KRISS). The 2012 data is plotted with error bars representing the expanded measurement uncertainty (k = 2).

7.2 Linearity of the angular acceleration standards

The linearity of the magnitude of both calibrated angular acceleration standards was determined at PTB using different angular acceleration amplitudes at the reference frequency of 16 Hz (acceleration range 14 rad/s² to 85 rad/s² for the Jewell ASMP-200, and 7 rad/s² to 127 rad/s² for the B&K 4381-ROT). The results indicated that the sensitivity of both angular accelerometers could be considered as constant, i.e. as independent from the angular acceleration amplitude (see Figures 5 and 6).

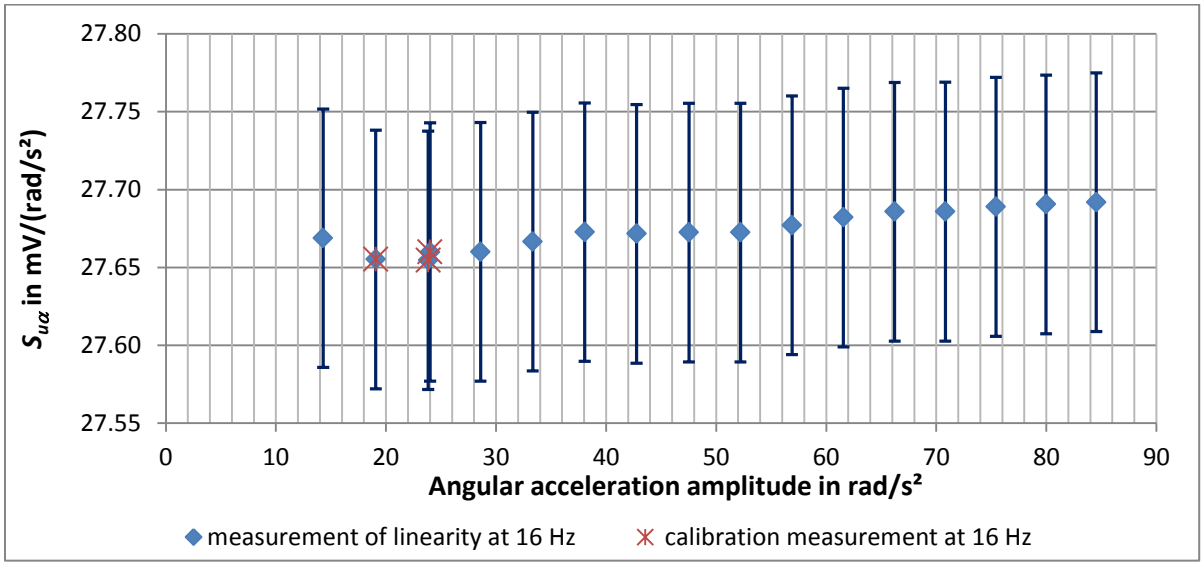

Figure 5: Linearity of the magnitude $S_{u\alpha}$ of the complex voltage sensitivity $\underline{S}_{u\alpha}$ of the Jewell ASMP-200 at 16 Hz with expanded measurement uncertainty (k = 2).

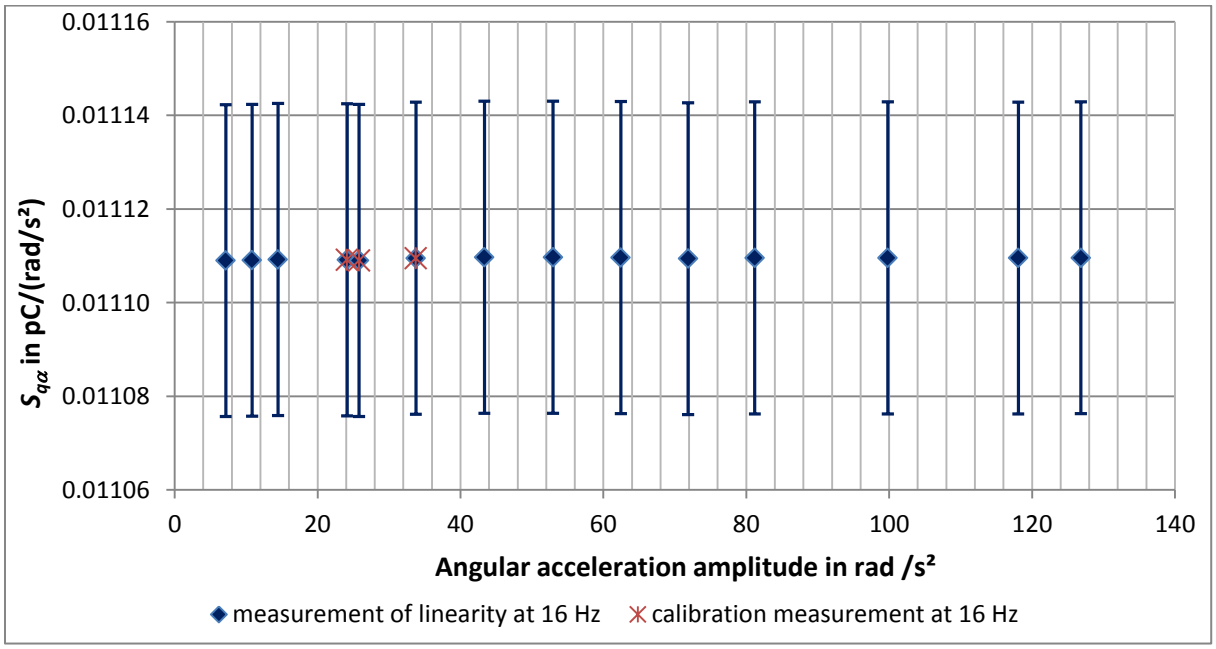

Figure 6: Linearity of the magnitude $S_{q\alpha}$ of the complex charge sensitivity $\underline{S}_{q\alpha}$ of the B&K type 4381-ROT at 16 Hz with expanded measurement uncertainty (k = 2).

7.3 Results for the magnitude of the complex sensitivity

7.3.1 Single-ended angular accelerometer Jewell, type ASMP-200, SN 50563, in the frequency range of 0.4 Hz to 100 Hz

Table 3a shows the magnitudes of the complex voltage sensitivity of the angular accelerometer Jewell ASMP-200 as raw results measured by PTB and KRISS. The values measured by KRISS were found to be smaller than those measured at PTB. This difference was caused by the combined effects of the relatively high output impedance (4.79 kΩ) of the Jewell ASMP-200 angular accelerometer and the different input impedance of the different voltage measurement instruments used at PTB and KRISS. Whereas the input impedance of the PTB voltage instrument was 1 MΩ, that of the KRISS instrument was 0.4957 MΩ.

Although the technical protocol prepared for this comparison did not consider effects of the output impedance of the ASMP-200 angular accelerometer, it became obvious that the measured voltage sensitivity data in Table 3a should be corrected by compensating the influence of the input impedance of the different voltage measurements used. Hence, a systematic correction of the raw results presented in Table 3a was made according to the following formulas.

$$S_{u\alpha,\mathrm{PTB}} = S_{u\alpha,\mathrm{raw}} \cdot \left(1 + \frac{4.79\,\mathrm{k\Omega}}{1\,\mathrm{M\Omega}}\right) = S_{u\alpha,\mathrm{raw}} \cdot 1.00479 \qquad (1)$$

$$S_{u\alpha,\mathrm{KRISS}} = S_{u\alpha,\mathrm{raw}} \cdot \left(1 + \frac{4.79\,\mathrm{k\Omega}}{0.4957\,\mathrm{M\Omega}}\right) = S_{u\alpha,\mathrm{raw}} \cdot 1.0096 \qquad (2)$$

The corrected sensitivity values are listed in Table 3b and shown in Figure 7. The corrections were made for all subsequent evaluations. Figure 8 shows the deviation between the results of KRISS and PTB of the magnitude $S_{u\alpha}$ of the complex voltage sensitivity $\underline{S}_{u\alpha}$ for the uncorrected and the corrected results of the Jewell ASMP-200.

Table 3a: Calibration results (magnitude $S_{u\alpha}$ of the complex voltage sensitivity $\underline{S}_{u\alpha}$) of PTB and KRISS, as reported to the BIPM, for the Jewell ASMP-200 with expanded measurement uncertainty (k = 2).

	PTB		**KRISS**	
Frequency in Hz	$S_{u\alpha,\,\mathrm{raw}}$ in mV/(rad/s²)	Exp. Uncertainty in %	$S_{u\alpha,\,\mathrm{raw}}$ in mV/(rad/s²)	Exp. Uncertainty in %
0.4	27.350	0.30	27.138	0.50
0.5	27.310	0.30	27.127	0.50
0.63	27.280	0.30	27.116	0.30
0.8	27.258	0.30	27.111	0.30
1	27.247	0.30	27.087	0.30
1.25	27.238	0.30	27.096	0.30
1.6	27.232	0.30	27.110	0.30
2	27.232	0.30	27.106	0.30
2.5	27.231	0.30	27.113	0.30
3.15	27.232	0.30	27.132	0.30
4	27.279	0.30	27.143	0.30
5	27.289	0.30	27.165	0.30
6.3	27.311	0.30	27.208	0.30
8	27.341	0.30	27.238	0.30
10	27.407	0.30	27.292	0.30
12.5	27.496	0.30	27.338	0.30
16	27.661	0.30	27.421	0.30
20	27.892	0.30	27.689	0.30
25	28.227	0.30	28.461	0.30
31.5	28.686	0.30	28.718	0.40
40	29.151	0.30	29.383	0.40
50	29.064	0.30	29.302	0.30
63	27.061	0.30	27.137	0.30
80	21.624	0.30	22.126	0.40
100	15.085	0.30	15.560	0.50

Table 3b: Corrected calibration results (magnitude $S_{u\alpha}$ of the complex voltage sensitivity $\underline{S}_{u\alpha}$) of PTB and KRISS for the Jewell ASMP-200 with expanded measurement uncertainty (k = 2).

	PTB		**KRISS**	
Frequency in Hz	$S_{u\alpha}$ in mV/(rad/s²)	Exp. Uncertainty in %	$S_{u\alpha}$ in mV/(rad/s²)	Exp. Uncertainty in %
0.4	27.481	0.30	27.400	0.50
0.5	27.441	0.30	27.389	0.50
0.63	27.411	0.30	27.378	0.30
0.8	27.389	0.30	27.373	0.30
1	27.378	0.30	27.349	0.30
1.25	27.368	0.30	27.358	0.30
1.6	27.362	0.30	27.372	0.30
2	27.362	0.30	27.368	0.30
2.5	27.361	0.30	27.375	0.30
3.15	27.362	0.30	27.394	0.30
4	27.410	0.30	27.405	0.30
5	27.420	0.30	27.427	0.30
6.3	27.442	0.30	27.471	0.30
8	27.472	0.30	27.501	0.30
10	27.538	0.30	27.556	0.30
12.5	27.628	0.30	27.602	0.30
16	27.793	0.30	27.686	0.30
20	28.026	0.30	27.956	0.30
25	28.362	0.30	28.736	0.30
31.5	28.823	0.30	28.995	0.40
40	29.291	0.30	29.667	0.40
50	29.203	0.30	29.585	0.30
63	27.191	0.30	27.399	0.30
80	21.728	0.30	22.340	0.40
100	15.157	0.30	15.710	0.50

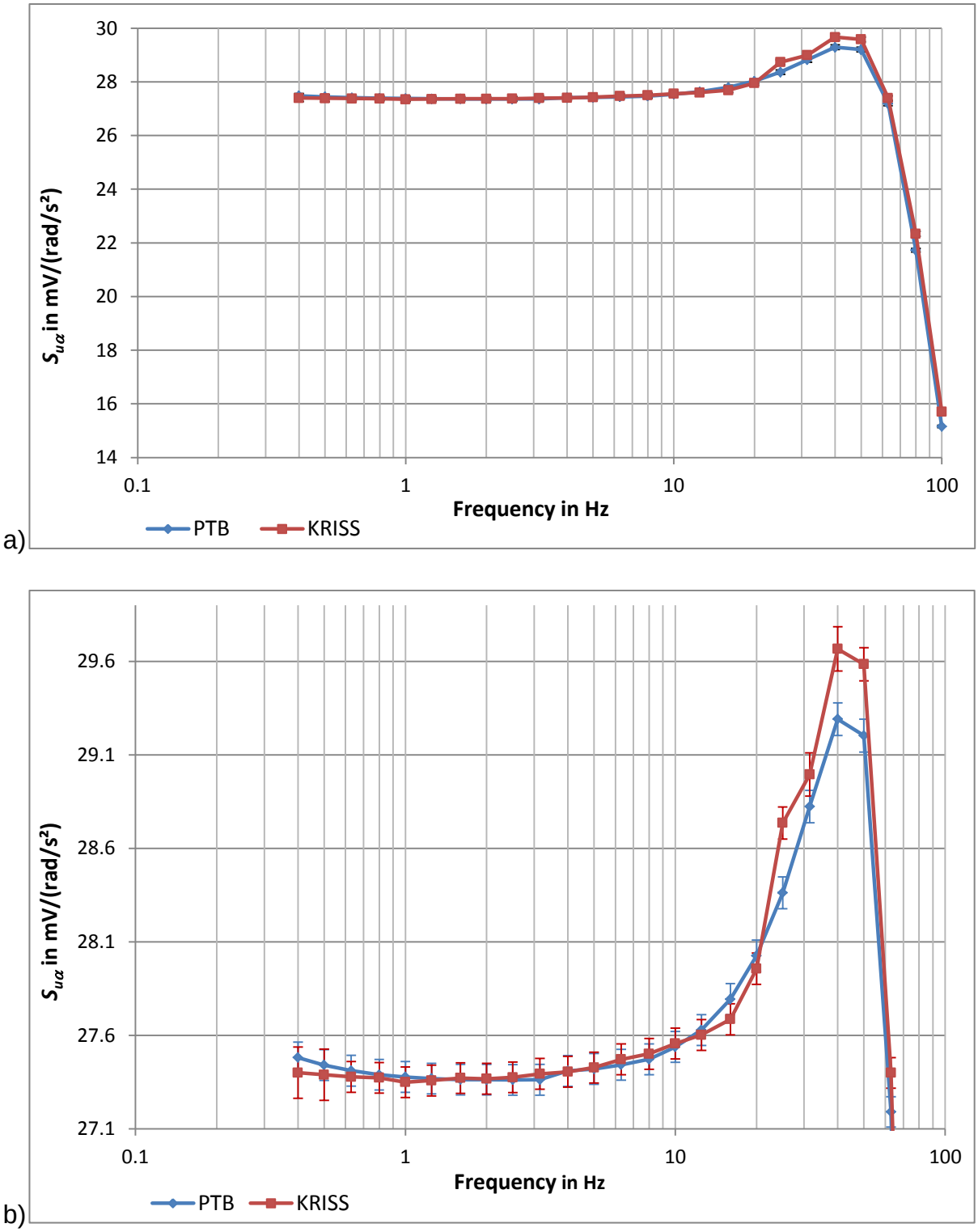

Figure 7: Magnitude $S_{u\alpha}$ of the complex voltage sensitivity $\underline{S}_{u\alpha}$ of the Jewell ASMP-200 in the frequency range of 0.4 Hz to 100 Hz with error bars representing the expanded measurement uncertainty (k = 2). These are the corrected values included in Table 3b.

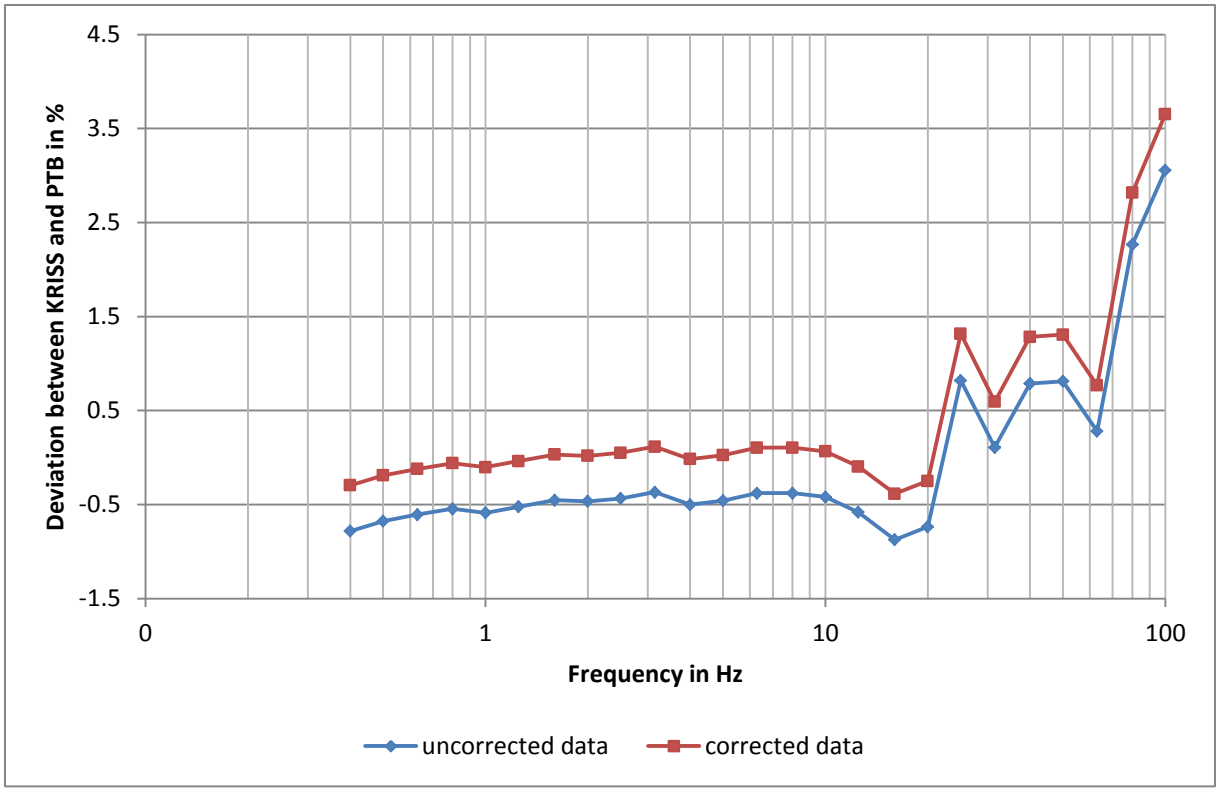

Figure 8: Deviation between the results of KRISS and PTB of the magnitude $S_{u\alpha}$ of the complex voltage sensitivity $\underline{S}_{u\alpha}$ for the uncorrected and corrected results of the Jewell ASMP-200 in the frequency range of 0.4 Hz to 100 Hz.

7.3.2 Back-to-back angular accelerometer B&K, type 4381-ROT, SN 30001, in the frequency range of 1 Hz to 1000 Hz

The calibration results of PTB and KRISS for the magnitude $S_{q\alpha}$ of the complex charge sensitivity $\underline{S}_{q\alpha}$ of the B&K 4381-ROT are listed in Table 4 and shown in Figure 9.

As the angular accelerometer B&K 4381-ROT is a charge accelerometer which was used with the NMI's charge amplifiers of low output impedance ≤1 Ω, a systematic correction as in equation (1) or (2) was not necessary.

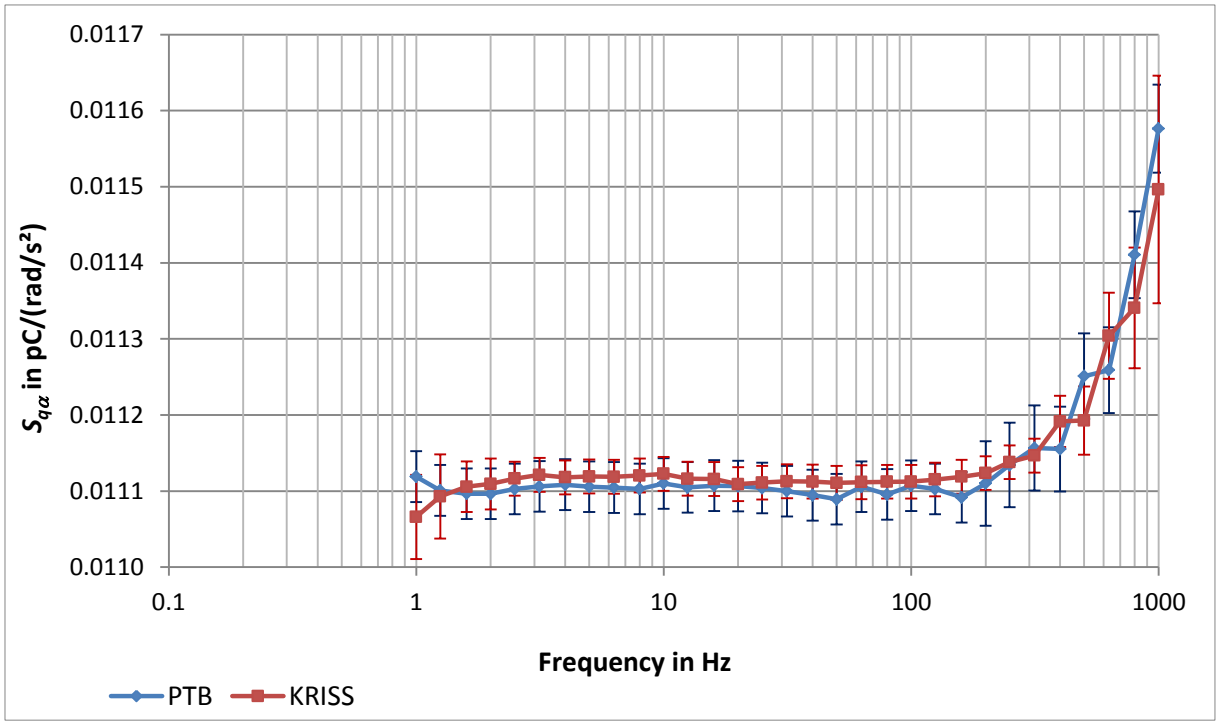

Figure 9: Magnitude $S_{q\alpha}$ of the complex charge sensitivity $\underline{S}_{q\alpha}$ of the B&K 4381-ROT of PTB and KRISS in the frequency range of 1 Hz to 1000 Hz with error bars representing the expanded measurement uncertainty (k = 2).

Table 4: Calibration results (magnitude $S_{q\alpha}$ of the complex charge sensitivity $\underline{S}_{q\alpha}$) of PTB and KRISS for the B&K 4381-ROT with expanded measurement uncertainty (k = 2).

PTB			**KRISS**	
Frequency in Hz	$S_{q\alpha}$ in pC/(rad/s²)	Exp. Uncertainty in %	$S_{q\alpha}$ in pC/(rad/s²)	Exp. Uncertainty in %
1	0.011119	0.30	0.011066	0.50
1.25	0.011101	0.30	0.011093	0.50
1.6	0.011097	0.30	0.011106	0.30
2	0.011096	0.30	0.011109	0.30
2.5	0.011103	0.30	0.011116	0.20
3.15	0.011106	0.30	0.011121	0.20
4	0.011108	0.30	0.011118	0.20
5	0.011106	0.30	0.011119	0.20
6.3	0.011105	0.30	0.011119	0.20
8	0.011103	0.30	0.011120	0.20
10	0.011110	0.30	0.011123	0.20
12.5	0.011105	0.30	0.011116	0.20
16	0.011107	0.30	0.011116	0.20
20	0.011107	0.30	0.011109	0.20
25	0.011104	0.30	0.011111	0.20
31.5	0.011100	0.30	0.011113	0.20
40	0.011095	0.30	0.011112	0.20
50	0.011089	0.30	0.011111	0.20
63	0.011106	0.30	0.011112	0.20
80	0.011096	0.30	0.011112	0.20
100	0.011107	0.30	0.011112	0.20
125	0.011103	0.30	0.011115	0.20
160	0.011092	0.30	0.011119	0.20
200	0.011110	0.50	0.011124	0.20
250	0.011134	0.50	0.011138	0.20
315	0.011157	0.50	0.011147	0.20
400	0.011155	0.50	0.011192	0.30
500	0.011251	0.50	0.011193	0.40
630	0.011259	0.50	0.011304	0.50
800	0.011410	0.50	0.011341	0.70
1000	0.011576	0.50	0.011496	1.30

7.4 Results for the phase shift of the complex sensitivity

7.4.1 Single-ended angular accelerometer Jewell, type ASMP-200, SN 50563, in the frequency range of 0.4 Hz to 100 Hz

The calibration results for the phase shift $\Delta\varphi_{u\alpha}$ of the complex voltage sensitivity $\underline{S}_{u\alpha}$ of the Jewell ASMP-200 are listed in Table 5 and shown in Figure 10.

Table 5: Calibration results (phase shift $\Delta\varphi_{u\alpha}$ of the complex voltage sensitivity $\underline{S}_{u\alpha}$) of PTB and KRISS for the Jewell ASMP-200 with expanded measurement uncertainty (k = 2).

PTB			**KRISS**	
Frequency in Hz	Phase Shift in °	Exp. Uncertainty in °	Phase Shift in °	Exp. Uncertainty in °
0.4	-0.57	0.50	-0.55	0.30
0.5	-0.66	0.50	-0.64	0.30
0.63	-0.78	0.50	-0.78	0.20
0.8	-0.94	0.50	-0.92	0.20
1	-1.12	0.50	-1.12	0.20
1.25	-1.36	0.50	-1.35	0.20
1.6	-1.70	0.50	-1.69	0.20
2	-2.11	0.50	-2.08	0.20
2.5	-2.69	0.50	-2.58	0.20
3.15	-3.25	0.50	-3.29	0.20
4	-4.11	0.50	-4.08	0.20
5	-5.12	0.50	-5.08	0.20
6.3	-6.44	0.50	-6.45	0.20
8	-8.18	0.50	-8.05	0.20
10	-10.21	0.50	-10.07	0.20
12.5	-12.83	0.50	-12.57	0.20
16	-16.54	0.50	-16.13	0.20
20	-20.92	0.50	-20.17	0.20
25	-26.65	0.50	-25.42	0.20
31.5	-34.66	0.50	-34.78	0.20
40	-46.25	0.50	-45.30	0.20
50	-61.53	0.50	-60.41	0.20
63	-83.10	0.50	-83.28	0.20
80	-109.46	0.50	-107.68	0.20
100	-132.31	0.50	-130.72	0.30

a)

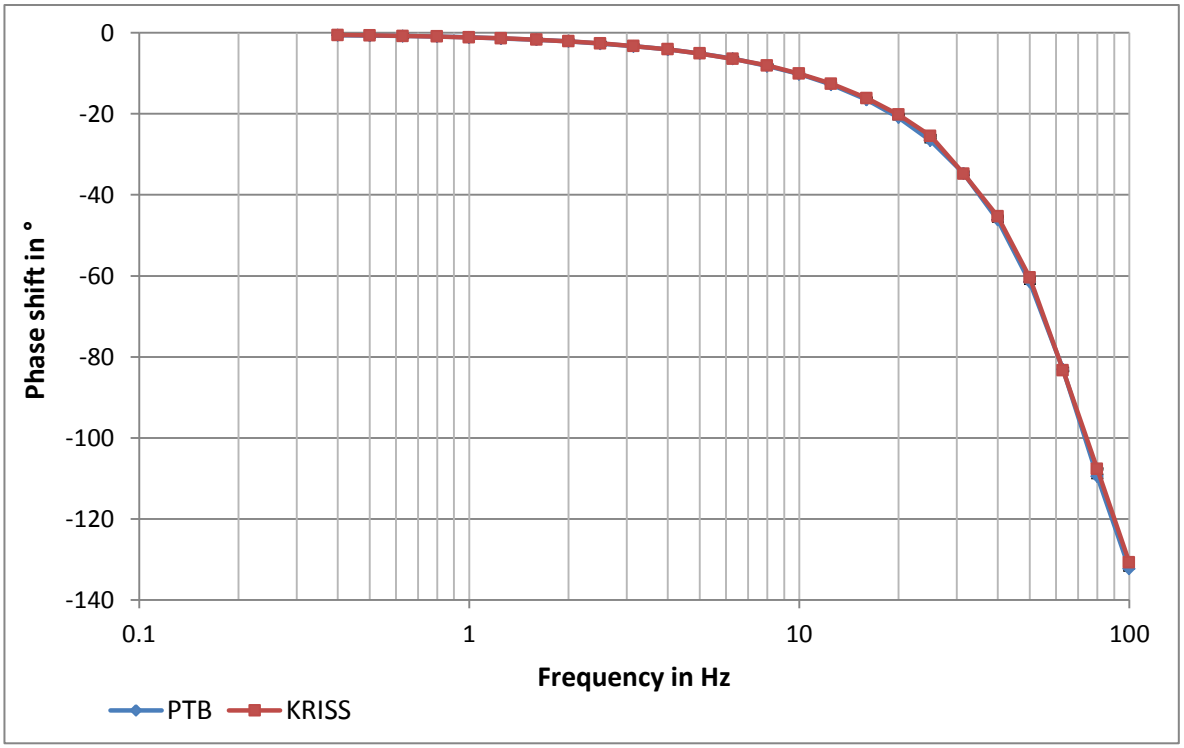

b)

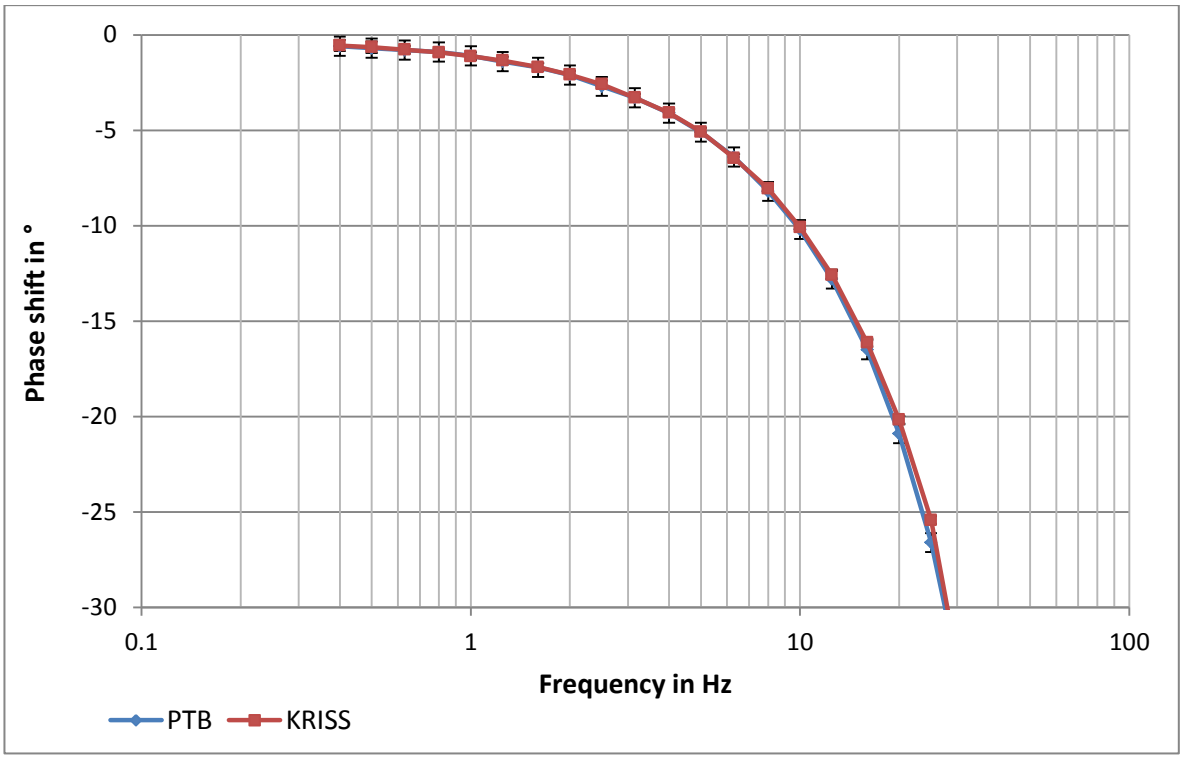

Figure 10: Phase shift $\Delta\varphi_{u\alpha}$ of the complex voltage sensitivity $\underline{S}_{u\alpha}$ of the Jewell ASMP-200 of PTB and KRISS in the frequency range of 0.4 Hz to 100 Hz with error bars representing the expanded measurement uncertainty (k = 2).

7.4.2 Back-to-back angular accelerometer B&K, type 4381-ROT, SN 30001, in the frequency range of 1 Hz to 1000 Hz

The calibration results for the phase shift $\Delta\varphi_{q\alpha}$ of the complex charge sensitivity $\underline{S}_{q\alpha}$ of the B&K 4381-ROT are listed in Table 6 and shown in Figure 11.

Table 6: Calibration results (phase shift $\Delta\varphi_{q\alpha}$ of the complex charge sensitivity $\underline{S}_{q\alpha}$) of PTB and KRISS for the B&K 4381-ROT with expanded measurement uncertainty (k = 2).

PTB			**KRISS**	
Frequency in Hz	Phase Shift in °	Exp. Uncertainty in °	Phase Shift in °	Exp. Uncertainty in °
1	-180.03	0.50	-180.08	0.20
1.25	-180.03	0.50	-180.12	0.20
1.6	-180.02	0.50	-180.09	0.10
2	-180.05	0.50	-180.04	0.10
2.5	-180.03	0.50	-180.03	0.10
3.15	-180.08	0.50	-180.06	0.10
4	-180.00	0.50	-180.04	0.10
5	-180.01	0.50	-180.04	0.10
6.3	-180.01	0.50	-180.04	0.10
8	-180.00	0.50	-180.01	0.10
10	-180.00	0.50	-180.03	0.10
12.5	-180.00	0.50	-180.03	0.10
16	-180.00	0.50	-180.03	0.10
20	-180.00	0.50	-180.05	0.10
25	-180.00	0.50	-180.01	0.10
31.5	-180.00	0.50	-180.03	0.10
40	-180.00	0.50	-180.03	0.10
50	-180.00	0.50	-180.05	0.10
63	-180.00	0.50	-180.03	0.10
80	-180.00	0.50	-180.03	0.10
100	-180.01	0.50	-180.04	0.10
125	-180.01	0.50	-180.04	0.10
160	-180.01	0.50	-180.04	0.10
200	-180.01	0.50	-180.05	0.10
250	-180.00	0.50	-180.07	0.10
315	-180.00	0.50	-180.07	0.10
400	-180.01	0.50	-180.13	0.20
500	-180.02	0.50	-180.12	0.30
630	-180.02	0.50	-180.16	0.30
800	-180.03	0.50	-180.13	0.30
1000	-180.04	0.50	-180.20	1.40

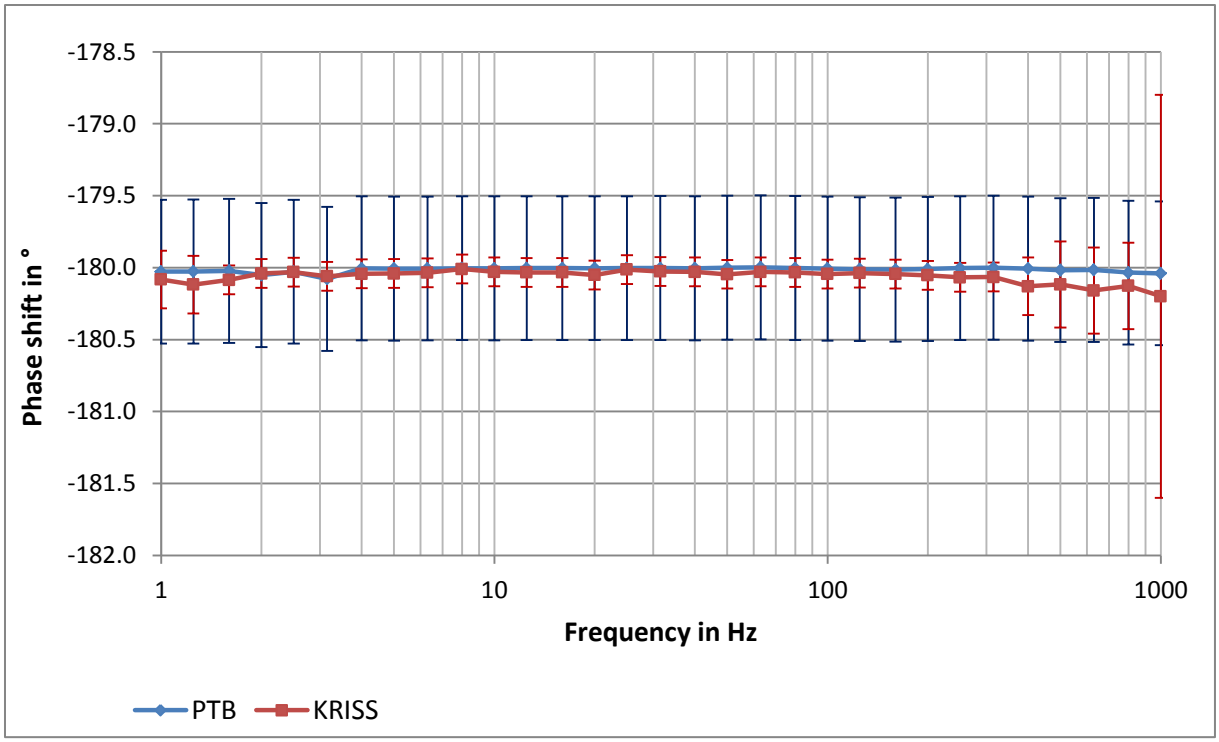

Figure 11: Phase shift $\Delta\varphi_{q\alpha}$ of the complex charge sensitivity $\underline{S}_{q\alpha}$ of the B&K 4381-ROT in the frequency range of 1 Hz to 1000 Hz with error bars representing the expanded measurement uncertainty (k = 2).

8 RESULTS OF THE COMPARISON

8.1 Degree of equivalence (DoE) between the participants

For each of the two angular acceleration standard accelerometers, the weighted mean (WM) of the results (measurement value *x* with associated measurement uncertainty *u*, at the frequency *f*) of the two laboratories has been determined according to:

$$\mathrm{WM} = \frac{1}{\sum_{i=1}^{2} 1/u^2(x_{i,f})} \sum_{i=1}^{2} x_{i,f} \,/ u^2(x_{i,f}) \tag{3}$$

$$u^2(\mathrm{WM}) = \frac{1}{\sum_{i=1}^{2} 1/u^2(x_{i,f})} \tag{4}$$

The index *i* denotes the participating NMI (i.e. PTB or KRISS).

In order to compare the individual results of the participating laboratories of this comparison with one another, the bilateral DoE of pairs of results with respect to each frequency was calculated. This DoE is each a pair of values comprising the difference

$$D_{\mathrm{NMI}} = x_{\mathrm{NMI}} - x_{\mathrm{WM}} \tag{5}$$

and its expanded uncertainty

$$U_{\mathrm{NMI}} = k \cdot \sqrt{u^2(x_{\mathrm{NMI}}) + u^2(x_{\mathrm{WM}})} \tag{6}$$

with a coverage factor of $k = 2$.

Note: All phase results for the back-to-back accelerometer were wrapped to 180°, since the polarity of its output is inverted relative to the single-ended accelerometer. As this is a question of convention rather than measurement uncertainty, this was not taken as a deviation.

8.1.1 Bilateral DoE for the magnitude of the complex voltage sensitivity of the single-ended angular accelerometer Jewell, type ASMP-200, SN 50563

The WM and the DoE are listed in Table 7 and shown in Figure 12 for the magnitude $S_{u\alpha}$ of the complex voltage sensitivity $\underline{S}_{u\alpha}$ of the Jewell ASMP-200.

Table 7: Bilateral DoE for the magnitude $S_{u\alpha}$ of the complex voltage sensitivity $\underline{S}_{u\alpha}$ of the Jewell ASMP-200 for PTB and KRISS.

Weighted Mean			*Degrees of Equivalence (Magnitude)*			
Frequency in Hz	WM in mV/(rad/s²)	U_{WM} in mV/(rad/s²)	D_{PTB} in mV/(rad/s²)	U_{PTB} in mV/(rad/s²)	D_{KRISS} in mV/(rad/s²)	U_{KRISS} in mV/(rad/s²)
0.4	27.4595	0.0706	0.022	0.109	-0.059	0.154
0.5	27.4272	0.0706	0.014	0.108	-0.038	0.154
0.63	27.3945	0.0581	0.017	0.101	-0.017	0.101
0.8	27.3810	0.0581	0.008	0.101	-0.008	0.101
1	27.3635	0.0580	0.015	0.101	-0.014	0.101
1.25	27.3630	0.0580	0.005	0.101	-0.005	0.101
1.6	27.3670	0.0581	-0.005	0.101	0.005	0.101
2.	27.3650	0.0580	-0.003	0.101	0.003	0.101
2.5	27.3680	0.0581	-0.007	0.101	0.007	0.101
3.15	27.3780	0.0581	-0.016	0.101	0.016	0.101
4	27.4075	0.0581	0.003	0.101	-0.002	0.101
5	27.4235	0.0582	-0.003	0.101	0.003	0.101
6.3	27.4565	0.0582	-0.014	0.101	0.015	0.101
8	27.4865	0.0583	-0.014	0.101	0.015	0.101
10	27.5470	0.0584	-0.009	0.101	0.009	0.101
12.5	27.6150	0.0586	0.013	0.101	-0.013	0.101
16	27.7393	0.0588	0.054	0.102	-0.053	0.102
20	27.9909	0.0594	0.035	0.103	-0.035	0.103
25	28.5466	0.0606	-0.185	0.104	0.189	0.105
31.5	28.8844	0.0693	-0.061	0.111	0.111	0.135
40	29.4242	0.0706	-0.133	0.113	0.243	0.138
50	29.3915	0.0624	-0.189	0.108	0.194	0.108
63	27.2942	0.0579	-0.103	0.100	0.105	0.101
80	21.9405	0.0527	-0.212	0.084	0.400	0.104
100	15.2958	0.0394	-0.139	0.060	0.414	0.088

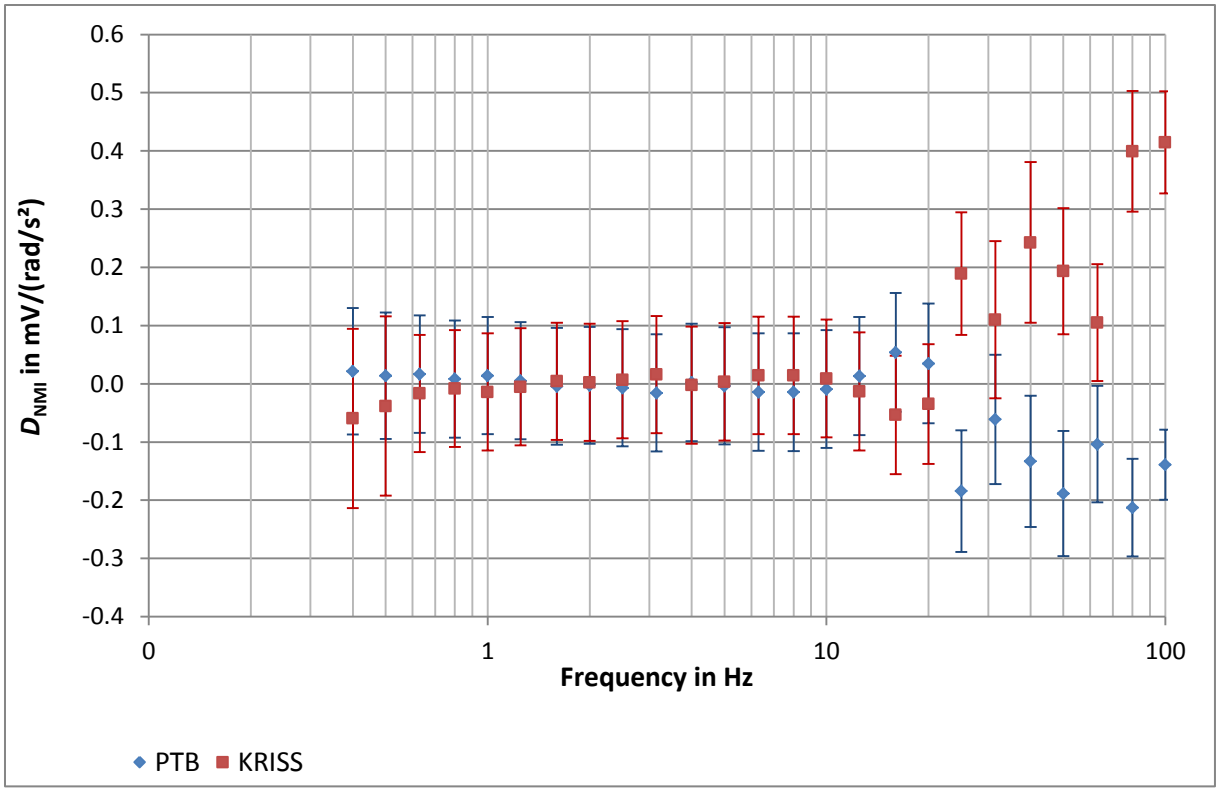

Figure 12: Bilateral DoE for the magnitude $S_{u\alpha}$ of the complex voltage sensitivity $\underline{S}_{u\alpha}$ of the Jewell ASMP-200 in the frequency range of 0.4 Hz to 100 Hz for PTB and KRISS.

8.1.2 Bilateral DoE for the magnitude of the complex charge sensitivity of the back-to-back angular accelerometer B&K, type 4381-ROT, SN 30001

The results for the WM and the DoE for the magnitude $S_{q\alpha}$ of the complex charge sensitivity $\underline{S}_{q\alpha}$ of the B&K 4381-ROT are listed in Table 8 and shown in Figure 12.

Table 8: Bilateral DoE for the magnitude $S_{q\alpha}$ of the complex charge sensitivity $\underline{S}_{q\alpha}$ of the B&K 4381-ROT for PTB and KRISS.

Weighted Mean			*Degrees of Equivalence (Magnitude)*			
Frequency in Hz	WM in pC/(rad/s²)	U_{WM} in pC/(rad/s²) x10^{-5}	D_{PTB} in pC/(rad/s²) x10^{-6}	U_{PTB} in pC/(rad/s²) x10^{-6}	D_{KRISS} in pC/(rad/s²) x10^{-6}	U_{KRISS} in pC/(rad/s²) x10^{-6}
1	0.010991	2.86	14.09	43.73	-38.76	62.27
1.25	0.011015	2.86	2.14	43.73	-5.93	62.38
1.6	0.011024	2.35	-4.36	40.68	4.37	40.80
2	0.011056	2.36	-6.69	40.72	6.71	40.81
2.5	0.011071	1.85	-9.23	38.06	4.11	28.92
3.15	0.011083	1.85	-10.57	38.08	4.71	28.93
4	0.011101	1.85	-6.96	38.10	3.10	28.92
5	0.011115	1.85	-9.10	38.11	4.06	28.93
6.3	0.011105	1.85	-9.54	38.10	4.25	28.92
8	0.011108	1.85	-12.02	38.09	5.36	28.93
10	0.011121	1.85	-8.73	38.12	3.89	28.93
12.5	0.011117	1.85	-7.77	38.11	3.46	28.92
16	0.011124	1.85	-6.11	38.12	2.72	28.92
20	0.011114	1.85	-1.45	38.11	0.65	28.90
25	0.011115	1.85	-4.89	38.10	2.18	28.91
31.5	0.011115	1.85	-8.84	38.09	3.94	28.91
40	0.011109	1.85	-12.06	38.07	5.38	28.91
50	0.011110	1.85	-15.07	38.06	6.72	28.90
63	0.011112	1.85	-3.94	38.11	1.75	28.91
80	0.011111	1.85	-11.24	38.08	5.01	28.91
100	0.011115	1.85	-3.68	38.11	1.64	28.91
125	0.011114	1.85	-8.45	38.10	3.76	28.92
160	0.011112	1.85	-18.62	38.07	8.31	28.92
200	0.011121	2.07	-11.72	59.26	1.88	30.36
250	0.011133	2.07	-3.41	59.38	0.55	30.40
315	0.011139	2.07	8.99	59.50	-1.44	30.42
400	0.011162	2.88	-26.80	62.73	9.71	44.21
500	0.011193	3.50	35.71	66.23	-22.62	56.85
630	0.011252	3.99	-22.47	68.93	22.65	69.18
800	0.011369	4.63	23.57	73.45	-45.64	91.91
1000	0.011550	5.40	10.40	79.09	-69.31	158.90

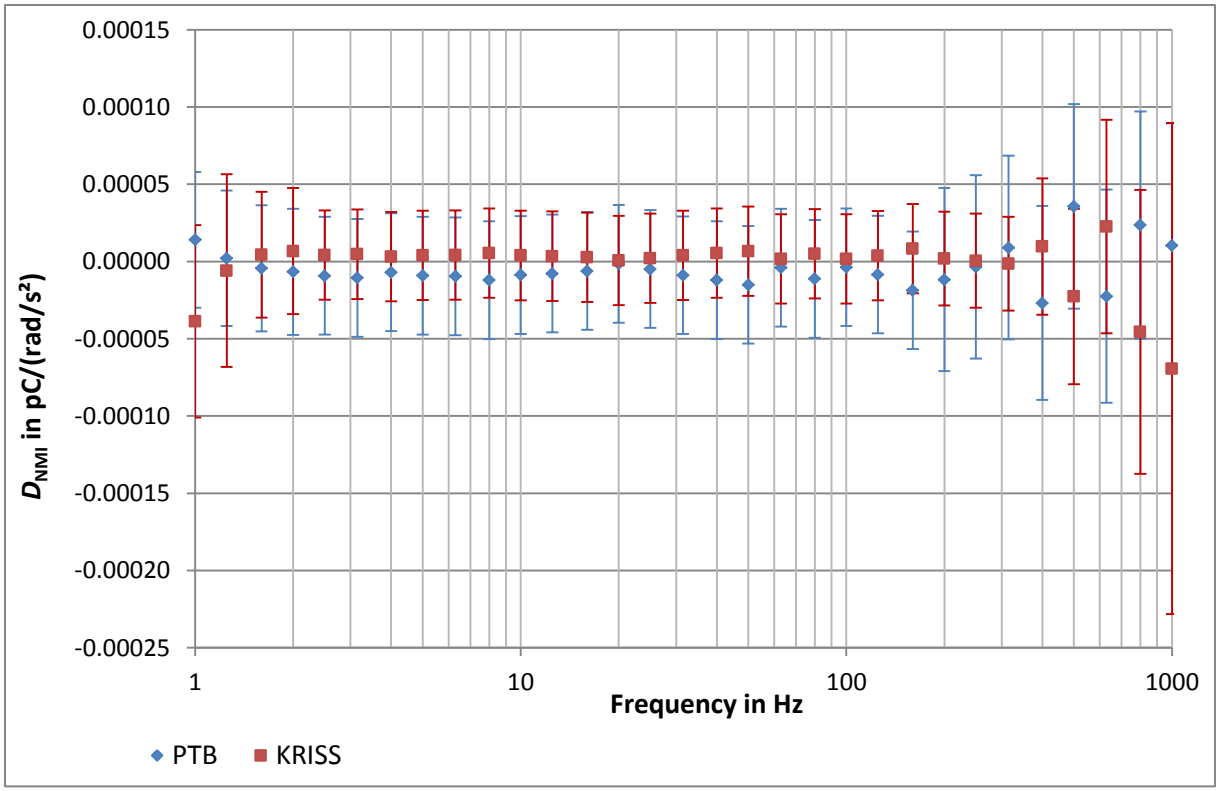

Figure 13: Bilateral DoE for the magnitude $S_{q\alpha}$ of the complex charge sensitivity $\underline{S}_{q\alpha}$ of the B&K 4381-ROT in the frequency range of 1 Hz to 1000 Hz for PTB and KRISS.

8.1.3 Bilateral DoE for the phase shift of the single-ended angular accelerometer Jewell, type ASMP-200, SN 50563

The WM and the DoE for the phase shift $\Delta\varphi_{u\alpha}$ of the complex voltage sensitivity $\underline{S}_{u\alpha}$ of the Jewell ASMP-200 are listed in Table 9 and shown in Figure 14.

Table 9: Bilateral DoE for the phase shift $\Delta\varphi_{u\alpha}$ of the complex voltage sensitivity $\underline{S}_{u\alpha}$ of the Jewell ASMP-200 for PTB and KRISS.

Weighted Mean			*Degrees of Equivalence (Phase Shift)*			
Frequency in Hz	WM in °	U_{WM} in °	D_{PTB} in °	U_{PTB} in °	D_{KRISS} in °	U_{KRISS} in °
0.4	-0.560	0.257	-0.015	0.562	0.005	0.395
0.5	-0.648	0.257	-0.014	0.562	0.005	0.395
0.63	-0.777	0.186	0.005	0.533	0.001	0.273
0.8	-0.925	0.186	-0.020	0.533	0.003	0.273
1	-1.121	0.186	0.003	0.533	0.000	0.273
1.25	-1.350	0.186	-0.008	0.533	0.001	0.273
1.6	-1.690	0.186	-0.013	0.533	0.002	0.273
2	-2.087	0.186	-0.021	0.533	0.003	0.273
2.5	-2.598	0.186	-0.091	0.533	0.015	0.273
3.15	-3.285	0.186	0.033	0.533	-0.005	0.273
4	-4.083	0.186	-0.025	0.533	0.004	0.273
5	-5.081	0.186	-0.036	0.533	0.006	0.273
6.3	-6.450	0.186	0.013	0.533	-0.002	0.273
8	-8.070	0.186	-0.114	0.533	0.018	0.273
10	-10.093	0.186	-0.113	0.533	0.018	0.273
12.5	-12.608	0.186	-0.220	0.533	0.035	0.273
16	-16.183	0.186	-0.352	0.533	0.056	0.273
20	-20.272	0.186	-0.649	0.533	0.104	0.273
25	-25.592	0.186	-1.058	0.533	0.169	0.273
31.5	-34.766	0.186	0.110	0.533	-0.018	0.273
40	-45.432	0.186	-0.815	0.533	0.130	0.273
50	-60.565	0.186	-0.965	0.533	0.154	0.273
63	-83.259	0.186	0.163	0.533	-0.026	0.273
80	-107.923	0.186	-1.533	0.533	0.245	0.273
100	-131.145	0.257	-1.168	0.562	0.421	0.395

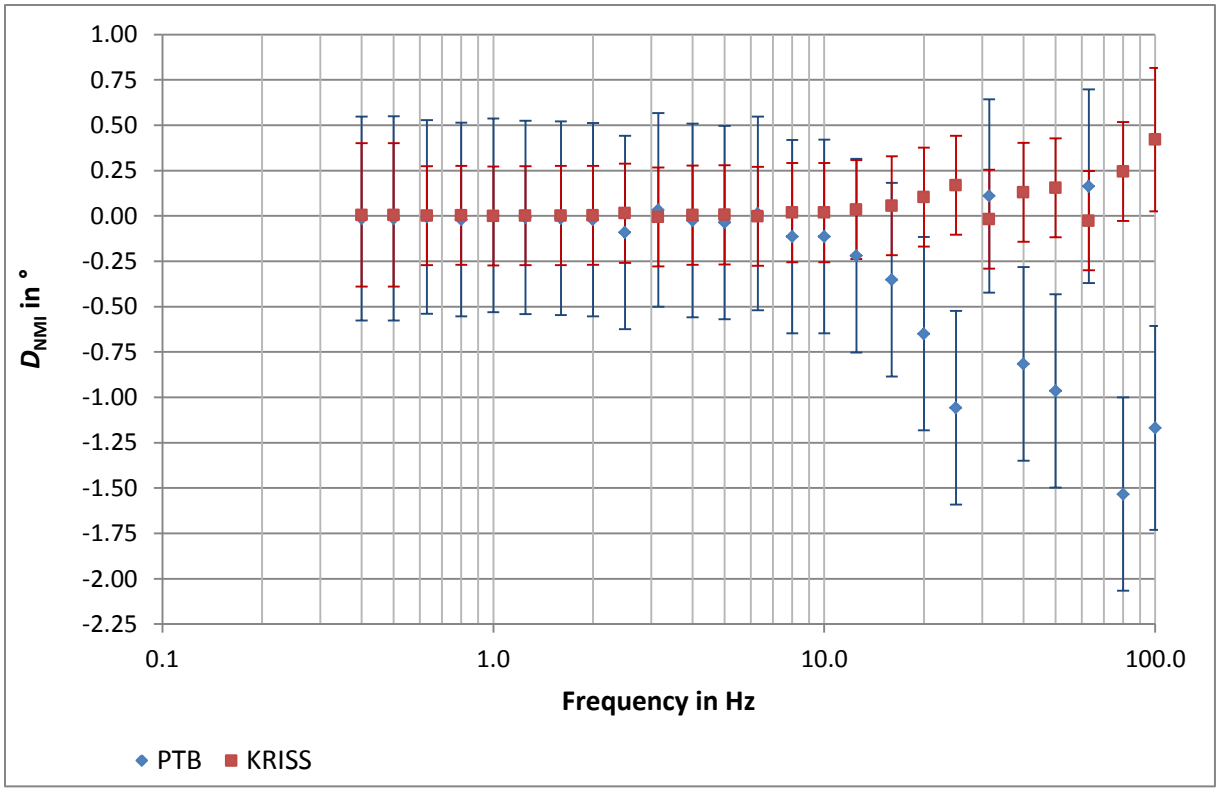

Figure 14: Bilateral DoE for the phase shift $\Delta\varphi_{u\alpha}$ of the complex voltage sensitivity $\underline{S}_{u\alpha}$ of the Jewell ASMP-200 in the frequency range of 0.4 Hz to 100 Hz for PTB and KRISS.

8.1.4 Bilateral DoE for the phase shift of the back-to-back angular accelerometer, B&K type 4381-ROT, SN 30001

The WM and the DoE for the phase shift $\Delta\varphi_{q\alpha}$ of the complex charge sensitivity $\underline{S}_{q\alpha}$ of the B&K 4381-ROT are listed in Table 10 and shown in Figure 15.

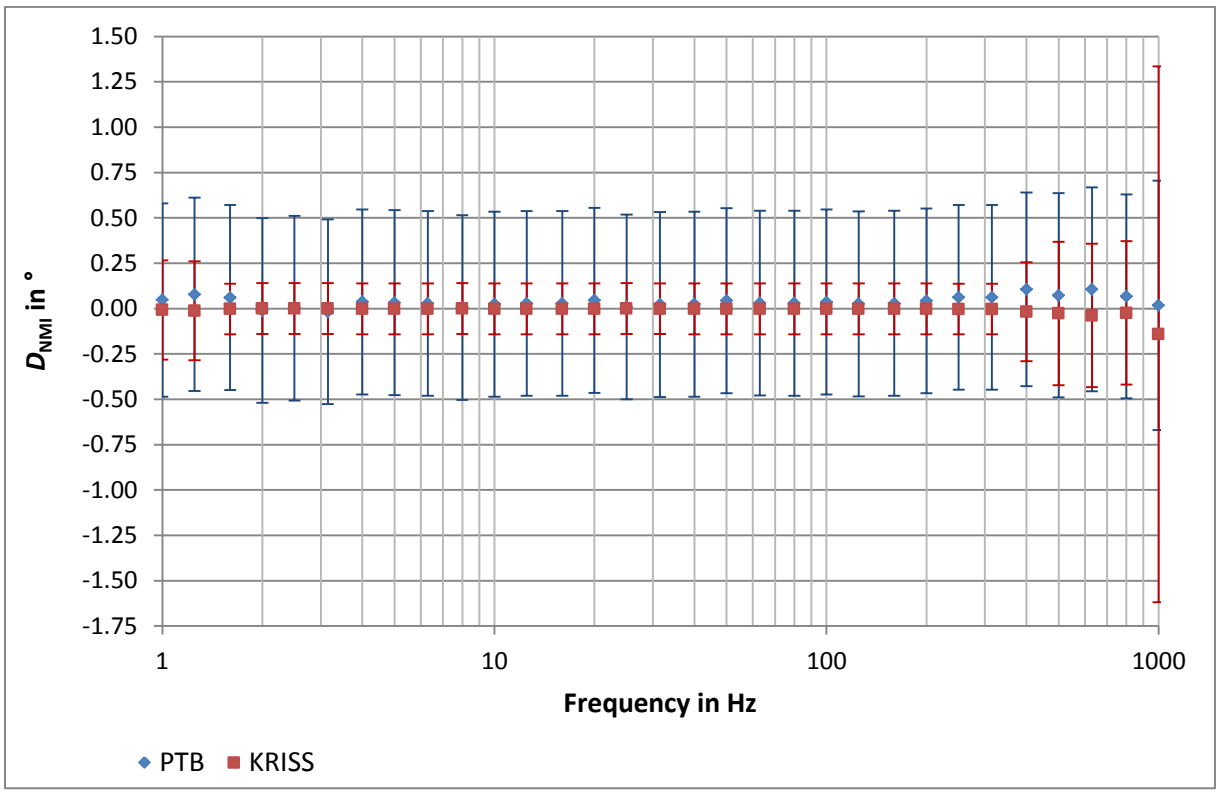

Figure 15: Bilateral DoE for the phase shift $\Delta\varphi_{q\alpha}$ of the complex charge sensitivity $\underline{S}_{q\alpha}$ of the B&K 4381-ROT in the frequency range of 1 Hz to 1000 Hz for PTB and KRISS.

Table 10: Bilateral DoE for the phase shift $\Delta\varphi_{q\alpha}$ of the complex charge sensitivity $\underline{S}_{q\alpha}$ of the B&K 4381-ROT for PTB and KRISS.

Weighted Mean			Degrees of Equivalence (Phase shift)			
Frequency in Hz	WM in °	U_{WM} in °	D_{PTB} in °	U_{PTB} in °	D_{KRISS} in °	U_{KRISS} in °
1	-180.075	0.186	0.047	0.533	-0.008	0.273
1.25	-180.105	0.186	0.079	0.533	-0.013	0.273
1.6	-180.083	0.098	0.061	0.510	-0.002	0.140
2	-180.041	0.098	-0.011	0.510	0.000	0.140
2.5	-180.030	0.098	0.002	0.510	0.000	0.140
3.15	-180.061	0.098	-0.017	0.510	0.001	0.140
4	-180.041	0.098	0.037	0.510	-0.001	0.140
5	-180.039	0.098	0.033	0.510	-0.001	0.140
6.3	-180.034	0.098	0.029	0.510	-0.001	0.140
8	-180.009	0.098	0.006	0.510	0.000	0.140
10	-180.029	0.098	0.024	0.510	-0.001	0.140
12.5	-180.032	0.098	0.028	0.510	-0.001	0.140
16	-180.032	0.098	0.029	0.510	-0.001	0.140
20	-180.049	0.098	0.045	0.510	-0.002	0.140
25	-180.012	0.098	0.009	0.510	0.000	0.140
31.5	-180.025	0.098	0.023	0.510	-0.001	0.140
40	-180.029	0.098	0.024	0.510	-0.001	0.140
50	-180.044	0.098	0.043	0.510	-0.002	0.140
63	-180.028	0.098	0.031	0.510	-0.001	0.140
80	-180.032	0.098	0.030	0.510	-0.001	0.140
100	-180.043	0.098	0.036	0.510	-0.001	0.140
125	-180.037	0.098	0.026	0.510	-0.001	0.140
160	-180.043	0.098	0.029	0.510	-0.001	0.140
200	-180.051	0.098	0.042	0.510	-0.002	0.140
250	-180.065	0.098	0.062	0.510	-0.002	0.140
315	-180.063	0.098	0.062	0.510	-0.002	0.140
400	-180.113	0.186	0.106	0.533	-0.017	0.273
500	-180.090	0.257	0.073	0.562	-0.026	0.395
630	-180.121	0.257	0.106	0.562	-0.038	0.395
800	-180.102	0.257	0.068	0.562	-0.024	0.395
1000	-180.057	0.471	0.018	0.687	-0.141	1.477

9 RESULTS OF THE MEASUREMENTS AND CONCLUSIONS

For the bilateral comparison between PTB and KRISS of calibrations of the magnitude and phase shift of the complex sensitivity of two investigated standard angular accelerometers, the sine-approximation method specified in ISO 16063-15 was applied.

Tables 3 to 6 contain the data for the two accelerometers as reported by the participating laboratories PTB and KRISS. For each laboratory, these data are the best estimate of the complex sensitivity (magnitude and phase shift) and their associated expanded uncertainty at frequency *f*.

For each of the two standard angular accelerometers and at each frequency *f*, a weighted mean value WM has been determined.

The bilateral degrees of equivalence ($D_{\mathrm{NMI}}, U_{\mathrm{NMI}}$) of each participating NMI were determined for the magnitude as well as for the phase shift of both accelerometers.

Tables 7 to 10 contain the results of the calibrated standard angular accelerometers.

9.1 Single-ended angular accelerometer Jewell, type ASMP-200, SN 50563

The angular accelerometer Jewell ASMP-200 operates on a torque balance principle; it is a servo-accelerometer. Due to the relatively high output impedance combined with differing input impedances of the voltage measurement systems of the two participants, a correction had to be applied to the raw calibration results (cf. Section 7.3.1, Table 3a and Table 3b). The data sets earlier submitted to BIPM were the raw results without any correction.

The degrees of equivalence (DoE) calculated for this angular accelerometer generally show a good agreement between the calibrations at KRISS and PTB for the magnitude in the frequency range from 0.4 Hz to 20 Hz (see Figures 7 and 12). The measurement results of the phase shift show good agreement in the frequency range from 0.4 Hz to 16 Hz and at the frequencies 31.5 Hz and 63 Hz (see Figure 14).

Considering the deviation observed for frequencies beyond 20 Hz, it should be noted that the natural (resonant) frequency of the angular accelerometer Jewell ASMP-200 is located at 68 Hz. This means that measurements in the frequency range 25 Hz to 100 Hz are not typical for this sensor and would not have been performed for a customer. However, these higher frequencies were included in the scope of scientific interest.

9.2 Back-to-back angular accelerometer B&K, type 4381-ROT, SN 30001

Excellent agreement was found for the measurement results for the magnitude and the phase shift of the complex charge sensitivity of the angular accelerometer B&K 4381-ROT for all frequencies in the measurement frequency range of 1 Hz to 1 kHz (cf. Figures 9 and 13 for the magnitude and Figures 10 and 15 for the phase shift).

REFERENCES

[1] ISO 16063-1:1998 “Methods for the calibration of vibration and shock transducers - Part 1: Basic concepts”

[2] ISO 16063-15:2006 “Methods for the calibration of vibration and shock transducers - Part 15: Primary vibration calibration by laser interferometry”

[3] ISO/IEC 17025:2005 “General requirements for the competence of testing and calibration laboratories”

[4] ISO/IEC Guide 98-3:2008 “Uncertainty of measurement - Part 3: Guide to the expression of uncertainty in measurement (GUM:1995)”

[5] Technical Protocol of the Bilateral Comparison in Primary Angular Vibration Calibration (2012-03-05)

ACKNOWLEDGEMENT

The KRISS working standard (Brüel & Kjaer type 4381-ROT, one of two artefacts) was kindly supplied by Brüel & Kjaer.

APPENDIX A

Measurement Budget of PTB for the PTB working standard Jewell, type ASMP-200, SN 50563 and the KRISS working standard Brüel & Kjaer, type 4381-ROT, SN 30001.

The Tables A-1 and A-2 list the standard uncertainties of the magnitude and phase shift of the complex voltage sensitivity of the PTB working standard Jewell, type ASMP-200, SN 50563.

The Tables A-3 and A-4 list the standard uncertainties of the magnitude and phase shift of the complex charge sensitivity of the KRISS working standard Brüel & Kjaer, 3 type 4381-ROT, SN 30001.

Table A-1: Standard uncertainties of the magnitude of the complex voltage sensitivity of the PTB working standard Jewell, type ASMP-200, SN 50563, frequency range 0.4 Hz to 100 Hz

Angular acceleration: 1 rad/s² to 500 rad/s²
Output voltage range: 15 mV to 4 V
Sample rate: 10 MS/s @ 12 Bit

Disturbing Component	**Comment**	**Distribution**	**Factor**	**Standard Uncertainty**
frequency of SAM	deviation of sample clock from generator clock	rectangular	1.73	5.77×10^{-5}
accelerometer voltage	sampling of HP3458A	rectangular	1.73	4.84×10^{-4}
velocity amplitude	uncertainty of traceability	normal	2	5×10^{-4}
harmonic distortion	mainly 1st harmonic	Steiner	1	8×10^{-6}
hum of voltage	typical 1mV	Steiner	1	1×10^{-4}
noise of voltage	Monte Carlo on influence to SAM duration 20 ms, Un= 1 mV	normal	2	1×10^{-5}
transverse motion	S(trans) ≤ 1%,transversal excitation ≤ 20 %	u-type	1.41	1.2×10^{-4}
temperature (estimated)		rectangular	1.73	1.5×10^{-5}
motion disturbance	drift, relative motion evaluation as velocity and period by period (estimated)	normal	2	1.5×10^{-4}
noise of Interferometer	noise level equiv. of 2 nm after demodulation ; Monte Carlo	normal	2	3×10^{-4}
asynchronous measurement	voltage/acceleration/voltage	rectangular	1.73	5.77×10^{-5}
residual influences		normal	2	1×10^{-4}
exp. standard deviation				8×10^{-4}
rel. standard uncertainty in %				0.1182
rel. comb. exp. uncertainty in %				0.2364
stated rel. comb. exp. uncertainty in %				0.3

Table A-2: Standard uncertainties of the phase shift of the complex voltage sensitivity of the PTB working standard Jewell, type ASMP-200, SN 50563, frequency range 0.4 Hz to 100 Hz

Angular acceleration: 1 rad/s² to 500 rad/s²
Output voltage range: 15 mV to 4 V
Sample rate: 10 MS/s @ 12 Bit

Disturbing Component	**Comment**	**Distribution**	**Factor**	**Standard uncertainty in °**
channel asynchronicity	all frequencies	normal	2	0.018
hum (50 Hz)	Monte Carlo, multiples of 20 ms are evaluated	normal	2	0.01
noise of accelerometer voltage output	Monte Carlo, SNR = 500	normal	2	0.01
transverse motion	*S*(trans) ≤ 1% transv. Excitation ≤ 20 %	u-type	1.41	0.1
delay of laser vibrometer	absolute correction 1.54 µs applied	rectangular	1.73	0.0208
noise of heterodyne interferometer channel	noise level equiv. of 0.02” after demodulation, Monte Carlo	normal	2	0.003
motion disturbance	drift, relative motion evaluation as velocity and period by period (estimated)	normal	2	0.01
temperature (estimated)		rectangular	1.73	0.01
residual influences		normal	2	0.1
exp. standard deviation	typical < 0.02°	normal	2	0.05
standard uncertainty				0.154
exp. uncertainty				0.31
stated exp. uncertainty				0.5

Table A-3: Standard uncertainties of the magnitude of the complex charge sensitivity of the KRISS working standard Brüel & Kjaer, type 4381-ROT, SN 30001, frequency range 1 Hz to 160 Hz

Angular acceleration: 1 rad/s² to 500 rad/s²
Output voltage range: 15 mV to 4 V
Sample rate: 10 MS/s @ 12 Bit

Disturbing Component	**Comment**	**Distribution**	**Factor**	**Standard uncertainty**
frequency of SAM	deviation of sample clock from generator clock	rectangular	1.73	5.77E-05
accelerometer voltage	sampling of HP3458A	rectangular	1.73	4.84E-04
velocity amplitude	uncertainty of traceability	normal	2	5E-04
harmonic distortion	mainly 1 st harmonic	Steiner	1	8E-06
hum of voltage	typical 1mV	Steiner	1	1E-04
noise of voltage	Monte Carlo on influence to SAM duration 20 ms, Un= 1 mV	normal	2	1E-05
transverse motion	*S*(trans) ≤ 1%, transv. excitation ≤ 20 %	u-type	1.41	1.2E-04
temperature (estimated)		rectangular	1.73	1.5E-05
motion disturbance	drift, relative motion, evaluation as velocity and period by period (estimated)	normal	2	1.5E-04
noise of Interferometer	noise level equiv. of 2 nm after demodulation; Monte Carlo	normal	2	3E-04
calibration of charge amplifier	including stability, reproducibility, method (black box)	normal	2	5E-04
residual influences		normal	2	1E-04
exp. standard deviation				8E-04
rel. standard uncertainty in %				0.1182
rel. comb. exp. uncertainty in %				0.2364
stated rel. comb. exp. uncertainty in %				0.3

Frequency range: 200 Hz to 1 kHz

Disturbing Component	Comment	Distribution	Factor	Standard uncertainty
frequency of SAM	deviation of sample clock from generator clock	rectangular	1.73	5.77E-05
accelerometer voltage	sampling of HP3458A	rectangular	1.73	4.84E-04
velocity amplitude	uncertainty of traceability	normal	2	5E-04
harmonic distortion	mainly 1 st harmonic	Steiner	1	8E-06
hum of voltage	typical 1mV	Steiner	1	1E-04
noise of voltage	Monte Carlo on influence to SAM duration 20 ms, Un= 1 mV	normal	2	1E-05
transverse motion	*S*(trans) ≤ 1% transv. excitation ≤ 20 %	u-type	1.41	1E-03
temperature (estimated)		rectangular	1.73	1.5E-05
motion disturbance	drift, relative motion evaluation as velocity and period by period (estimated)	normal	2	1.5E-04
noise of interferometer	noise level equiv. of 2 nm after demodulation ; Monte Carlo	normal	2	3E-04
asynchronous measurement	voltage/acceleration/voltage	rectangular	1.73	5.77E-05
residual influences		normal	2	1E-04
exp. standard deviation				8E-04
calibration of charge amplifier	including stability, reproducibility, method (black box)	normal	2	5E-04
rel. standard uncertainty in %				0.164
rel. comb. exp. uncertainty in %				0.328
stated rel. comb. exp. uncertainty in %				0.5

Table A-4: Standard uncertainties of the phase shift of the complex charge sensitivity of the KRISS working standard Brüel & Kjaer, type 4381-ROT, SN 30001, frequency range 1 Hz to 1 kHz

Angular acceleration: 1 rad/s² to 500 rad/s²
Output voltage range: 15 mV to 4 V
Sample rate: 10 MS/s @ 12 Bit

Disturbing Component	**Comment**	**Distribution**	**Factor**	**Standard uncertainty in °**
channel a-synchronicity	all frequencies	normal	2	0.018
hum (50 Hz)	Monte Carlo, multiples of 20 ms are evaluated	normal	2	0.0
noise of accelerometer voltage output	Monte Carlo, SNR = 500	normal	2	0.01
transverse motion	*S*(trans) ≤ 1%, transv. Excitation ≤ 20 %	u-type	1.41	0.1
delay of the laser vibrometer	absolute correction 1.54 µs applied	rectangular	1.73	0.0208
noise of heterodyne interferometer channel	noise level equiv. of 2 nm after demodulation, Monte Carlo	normal	2	0.003
motion disturbance	drift, relative motion, evaluation as velocity and period by period (estimated)	normal	2	0.01
temperature (estimated)		rectangular	1.73	0.01
residual influences		normal	2	0.1
exp. standard deviation	typical < 0.02°	normal	2	0.05
calibration of charge amplifier	including stability, reproducibility, method (black box)	normal	2	0,02
standard uncertainty				0.155
exp. uncertainty				0.31
stated exp. uncertainty				0.5

Appendix B:

Measurement Budget of KRISS for the PTB working standard Jewell, type ASMP-200, SN 50563 and the KRISS working standard Brüel & Kjaer, type 4381-ROT, SN 30001.

This appendix introduces distinctive features of the measurement model and uncertainty budgets of the complex sensitivity developed by the AUV team of KRISS. The evaluation method of the standard uncertainties of the magnitude and phase shift components of the complex sensitivity is based on the mathematical model for evaluating the frequency response function from the Fourier coefficients of the applied angular vibration and voltage output signals.

Measurement Model of Complex Sensitivity

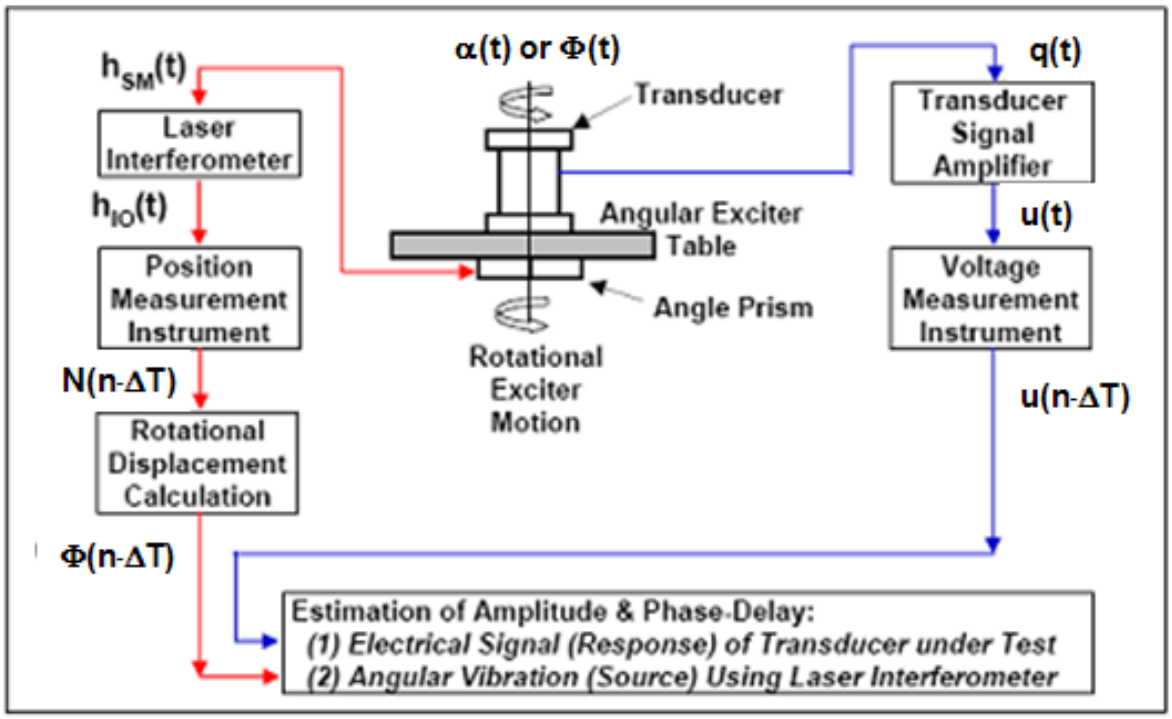

Figure B-1. Flow diagram of measured angular displacement and voltage output signals.

As shown in Figure B-1, two measurements, the angular displacement signal $\Phi(n\Delta T)$ and the voltage output signal $u(n\Delta T)$, are simultaneously sampled at each sampling interval ΔT. The discrete Fourier transform is exploited to evaluate the cosine and sine components $\{C_\Phi(m), S_\Phi(m); m = 1, 2, \ldots, M\}$ of the measured angular displacement signals over each period and the cosine and sine components $\{C_V(m), S_V(m); m = 1, 2, \ldots, M\}$ of the measured voltage output signals, respectively.

$$C_{\Phi}(m) = \frac{2}{N}\sum_{n=1}^{N_P}\Phi\left(((m-1)\cdot N_P + n)\Delta T\right)\cdot\cos\left(\frac{2\pi n}{N_P}\right)$$

$$S_{\Phi}(m) = \frac{2}{N}\sum_{n=1}^{N_P}\Phi\left(((m-1)\cdot N_P + n)\Delta T\right)\cdot\sin\left(\frac{2\pi n}{N_P}\right)$$

$$C_{V}(m) = \frac{2}{N}\sum_{n=1}^{N_P}V\left(((m-1)\cdot N_P + n)\Delta T\right)\cdot\cos\left(\frac{2\pi n}{N_P}\right)$$

$$S_{V}(m) = \frac{2}{N}\sum_{n=1}^{N_P}V\left(((m-1)\cdot N_P + n)\Delta T\right)\cdot\sin\left(\frac{2\pi n}{N_P}\right)$$

Both cosine and sine components are used to calculate the real and imaginary parts $R(m)$ and $I(m)$ of the complex sensitivity for each period in the same way of evaluating the frequency response function between input and output signals:

$$R(m) = \frac{C_{\Phi}(m)C_{V}(m) + S_{\Phi}(m)S_{V}(m)}{C_{\Phi}^2(m) + S_{\Phi}^2(m)},\ I(m) = \frac{-C_{\Phi}(m)S_{V}(m) + S_{\Phi}(m)C_{V}(m)}{C_{\Phi}^2(m) + S_{\Phi}^2(m)}$$

The mean values of the real and imaginary parts over the M periods are obtained as

$$R_M = \frac{1}{M}\sum_{m=1}^{M}R(m),\ I_M = \frac{1}{M}\sum_{m=1}^{M}I(m)$$

The magnitude and phase shift of the complex sensitivity at the calibration frequency f in reference to the angular displacement Φ are calculated as

$$S_{\Phi}(f) = \sqrt{R_M^2 + I_M^2},\ \Delta\varphi_{\Phi}(f) = \arctan\left(\frac{I_M}{R_M}\right)$$

Finally, the magnitude and phase shift of the complex sensitivity in reference to the applied angular acceleration α are evaluated as

$$S_\alpha(f) = \frac{1}{4\pi^2 f^2}\sqrt{R_M^2 + I_M^2},\ \Delta\varphi_\alpha(f) = \pi + \arctan\left(\frac{I_M}{R_M}\right)$$

UNCERTAINTY BUDGETS

The A-type relative standard uncertainty $u_{r,S}$ of the magnitude of the complex sensitivity in reference to the applied angular acceleration α is calculated as

$$\begin{aligned} u_{r,S}^2(R_M, I_M, f) &= u_{r,S}^2(R_M, I_M) + 4u_r^2(f) \\ &= \frac{R_M^2}{R_M^2 + I_M^2}u^2(R_M) + \frac{I_M^2}{R_M^2 + I_M^2}u^2(I_M) + \frac{2R_M I_M}{R_M^2 + I_M^2}u^2(R_M, I_M) + 4u_r^2(f) \end{aligned}$$

where $u(R_M)$ and $u(I_M)$ denote the standard uncertainties of the real and imaginary parts R_M and I_M evaluated from the series of the real and imaginary parts $\{R(m), I(m); m = 1, 2, \ldots, M\}$, and $u^2(R_M, I_M)$ denote their covariance normalized by the sample size M. The symbol $u_r(f)$ denotes the relative standard uncertainty of the calibration frequency f.

In a similar way, the A-type standard uncertainty $u_{r,\varphi}$ of the phase shift of the complex sensitivity is calculated as

$$u_{r,\varphi}^2(R_M, I_M) = \frac{I_M^2}{R_M^2 + I_M^2}u^2(R_M) + \frac{R_M^2}{R_M^2 + I_M^2}u^2(I_M) - \frac{2R_M I_M}{R_M^2 + I_M^2}u^2(R_M, I_M)$$

As a result, the relative combined standard uncertainties $u_{r,c}(S_\alpha)$ and $u_c(\Delta\varphi)$ of the magnitude and phase of the complex sensitivity is calculated respectively as follows:

$$u_{r,c}\left(S_\alpha\right)=\left\{u_{r,S}^2\left(R_M,I_M\right)+4u_r^2\left(f\right)+u_r^2\left(\Phi\right)+u_r^2\left(V\right)+u_r^2\left(S_{RE}\right)\right\}^{1/2},$$

$$u_c\left(\Delta\varphi\right)=\left\{u_{\Delta\varphi}^2\left(R_M,I_M\right)+u_{\Delta\varphi}^2\left(\Phi\right)+u_{\Delta\varphi}^2\left(V\right)+u_{\Delta\varphi}^2\left(S_{RE}\right)\right\}^{1/2}.$$

The uncertainty components contributing to the relative combined standard uncertainty $u_{r,c}(S_\alpha)$ of the magnitude of the complex sensitivity are as follows:

$u_{r,S}(R_M,I_M)$: relative standard uncertainty of magnitude of complex sensitivity

$u_r(f)$: relative uncertainty of frequency readings

$u_r(\Phi)$: relative standard uncertainty of measured angular displacement by laser interferometry, which includes further uncertainty components,

$$u_r\left(\Phi\right)=\left\{u_{r,MA}^2+c_{FS}^2\cdot u_{AP}^2+u_{r,P}^2+c_{PC}^2\cdot u^2\left(N\right)+u_{r,BA}^2\right\}^{1/2}$$

$u_{r,MA}$: relative standard uncertainty of angle prism misalignment, $u_{r,MA}$= 9.56 10^{-8}.

u_{AP}: standard uncertainty of calibrated angle prism (evaluated by the linear regression model of the calibration data sheet)

c_{FS}: sensitivity coefficient of angular displacement, $c_{FS} = 1/\Phi$

$u_{r,P}$: relative standard uncertainty of compensation error of digital filter (ZMI 4004 measurement board), $u_{r,P}$ = 0.0001

c_{PC}: sensitivity coefficient of ZMI 4004 position count

$u(N)$: standard uncertainty of ZMI 4004 position counter, $u(N)$ = 1.64 LSB

$u_{r,BA}$: relative standard uncertainty of the background angular displacement

$u_r(V)$: relative standard uncertainty of measured voltage (or charge) output of angular vibration transducer under calibration, which includes further uncertainty components,

$$u_r\left(V\right)=\left\{u_{r,VC}^2+u_{r,GC}^2+u_{r,QE}^2+u_{r,CC}^2+u_{r,CN}^2\right\}^{1/2}$$

$u_{r,VC}$: relative standard uncertainty of AC/DC reference voltage source , $u_{r,VC}$ = 54 ppm

$u_{r,GC}$: relative standard uncertainty of compensated gain of AD converter (evaluated from the linear regression model)

$u_{r,QE}$: relative standard uncertainty of quantization error of AD converter

$u_{r,CA}$: relative standard uncertainty of gain of calibrated charge amplifier (in case of voltage output transducers, $u_{r,CA} = 0$)

$u_{r,CN}$: relative standard uncertainty of combined background noise level of charger amplifier and AD converter (in case of voltage output transducers under calibration, the background noise level of the AD converter is considered)

$u_r(S_{RE})$: relative repeatability standard deviation of magnitude of complex sensitivities (obtained from the regularly repeated tests)

The uncertainty components contributed to the combined standard uncertainties $u_c(\Delta\varphi)$ of the phase shift of the complex sensitivity are as follows:

$u_{\Delta\varphi}(R_M, I_M)$: standard uncertainty of phase shift of complex sensitivity,

$u_{\Delta\varphi}(\Phi)$: standard uncertainty of phase shift (accompanied with angular displacement by laser interferometry),

$$u_{\Delta\varphi}(\Phi) = \left\{ c_{AU}^2 \cdot u_r^2(\Phi) + u_{\Delta\varphi,ZMI}^2 \right\}^{1/2}$$

c_{AU}: sensitivity coefficient, $c_{AU} = 180/\pi$

$u_r(\Phi)$:relative standard uncertainty of measured angular displacement by laser interferometry

$u_{\Delta\varphi,ZMI}$: standard uncertainty of effective time delay of optic receiver of ZMI 4004 position measurement board.

$u_{\Delta\varphi}(V)$: standard uncertainty of phase shift (accompanied with voltage or charge output measurements),

$$u_{\Delta\varphi}(V) = \left\{ c_{AU}^2 \cdot u_r^2(V) + u_{\Delta\varphi,CA}^2 \right\}^{1/2}$$

$u_r(V)$: relative standard uncertainty of measured voltage or charge output of angular vibration transducer under calibration

$u_{\Delta\varphi,CA}$: standard uncertainty of phase shift of calibrated charge amplifier

$u_{\Delta\varphi}(S_{RE})$: repeatability standard deviation of phase shift of complex sensitivities (obtained from regularly repeated tests).

The Tables B-1 and B-2 show the uncertainty budgets of the magnitude and phase shift of the complex voltage sensitivity at the calibration frequency of 8 Hz. The

uncertainty budgets over the frequency range of 0.4 Hz to 200 Hz are separately submitted as the excel file (20130206_KRISS_Uncertainty_Budget. xlsx) attached with this report since they cannot fit into one page.

The Tables B-3 and B-4 show the uncertainty budgets of the magnitude and phase shift of the complex charge sensitivity at the calibration frequency of 80 Hz. The uncertainty budgets over the frequency range of 1 Hz to 1 kHz are separately submitted as the Excel file (20130206_KRISS_Uncertainty_Budget.xlsx) attached with this report since they cannot fit into one page.

Table B-1: Uncertainty budget of the magnitude of the complex charge sensitivity at the calibration frequency of 8 Hz:
acceleration angle $\Phi_{peak} = 3.207\times10^{-2}$°, output voltage $V_{peak} = 1.11$ V.

Uncertainty components	Description	Standard uncertainty u	Probability distribution	Sensitivity coefficient: c	Contribute damount $c\cdot u_r$ in %	Degree of freedom
$u_r(f)$	relative uncertainty of frequency readings	1.5×10^{-12}	uniform	2	3.0×10^{-10}	∞
$u_{r,S}(R_M, I_M)$	relative std. uncertainty of the magnitude of the complex sensitivity	1.743×10^{-4}	normal	1	1.743×10^{-2}	48
$u_r(\Phi)$	relative std. uncertainty of the magnitude of the angular displacement	1.00×10^{-4}	-	1	1.00×10^{-2}	
$u_{r,MA}$	misalignment of angle prism	9.56×10^{-8}	-	1	9.56×10^{-6}	-
$u_{r,AP}$	calibration uncertainty of angle prism	2.768×10^{-6}°	normal	$1/\Phi$	8.63×10^{-5}	61
$u_{r,P}$	compensation uncertainty of the digital filter (ZMI 4004)	1.00×10^{-4}	-	1	1.00×10^{-2}	-
$u(N)$	counter uncertainty of ZMI 4004	1.64 LSB	uniform	6.43E-06/Φ	3.29×10^{-4}	∞
$u_{r,BA}$	relative std. uncertainty of background angular vibration level	1.33×10^{-7}	normal	1	1.33×10^{-5}	∞
$u_r(V)$	relative std. uncertainty of the magnitude of the	5.94×10^{-5}	-	1	5.94×10^{-3}	

	voltage output					
$u_{r,VC}$	relative std. uncertainty of AC/DC calibration source	54 ppm	normal	1	5.4×10^{-3}	∞
$u_{r,GC}$	relative std. uncertainty of compensated gain of AD converter	8.96×10^{-5} Vpeak	normal	$1/V$	2.33×10^{-3}	42
$u_{r,QE}$	relative std. uncertainty of quantization resolution of AD converter	8.81×10^{-6}	uniform	1	8.81×10^{-4}	∞
$u_{r,CA}$	relative std. uncertainty of the gain of calibrated charge amplifier	0	normal	1	0	
$u_{r,CN}$	relative std. uncertainty of charge amplifier background noise	5.47×10^{-7}	normal	1	5.47×10^{-5}	50
$u_r(S_{RE})$	relative std. uncertainty of the magnitude repeatability of complex sensitivity	1.0×10^{-3}	normal	1	1.0×10^{-1}	
$u_{r,c}(S)$	combined uncertainty	1.02×10^{-1}	-	1	1.02×10^{-1}	
$U_r(S)$	expanded uncertainty (k = 2, L.C. = 95 %)	0.204	-	1	0.204	

Table B-2: Uncertainty budget of the phase of the complex charge sensitivity at the calibration frequency of 8 Hz:
acceleration angle $\Phi_{peak} = 3.207\times10^{-2}$°, output voltage $V_{peak} = 1.11$ V.

Uncertainty components	Description	Standard uncertainty u	Probability distribution	Sensitivity coefficient c	Contribute damount $c\cdot u_r$ in °	Degree of freedom
$u_{\Delta\varphi}(R_M, I_M)$	standard uncertainty of the phase shift of the complex sensitivity	1.0×10^{-2}°	normal	1	1.0×10^{-2}	48
$\Delta\varphi\,(\Phi)$	standard uncertainty of the phase shift of the angular displacement	5.73×10^{-3}°	uniform	1	5.73×10^{-3}	
$c_{AU}{*}u_r(\Phi)$	effect of relative std. uncertainty of the magnitude of angular displacement measurement	1.0×10^{-4}	-	$180/\pi$	5.73×10^{-3}	∞
$u_{\Delta\varphi,ZMI}$	effective time delay of optic receiver of ZMI 4004 board	2.02×10^{-8} s	uniform	$360f$	5.82×10^{-5}	∞
$\Delta\varphi\,(V)$	relative uncertainty of the phase shift of the voltage output	3.40×10^{-3}°	normal	1	3.40×10^{-3}	
$c_{AU}{*}u_r(V)$	effect of relative std. uncertainty of the magnitude of voltage output measurement	5.934×10^{-5}	normal	$180/\pi$	3.40×10^{-3}	∞
$u_{\Delta\varphi,CA}$	standard uncertainty of the Phase shift of calibrated charge amplifier	0°	normal	1	0	50
$u_r(S_{RE})$	relative std. uncertainty of the phase repeatability of complex sensitivity	5.73×10^{-2}°	normal	1	5.73×10^{-2}	
$u_{r,c}(S)$	combined uncertainty	5.86×10^{-2}°	-	1	5.86×10^{-2}	
$U_r(S)$	expanded uncertainty (k = 2, L.C. = 95 %)	0.117°	-	1	0.117	

Table B-3: Uncertainty budget of the magnitude of the complex charge sensitivity at the calibration frequency of 80 Hz:
acceleration angle $\Phi_{peak} = 3.207\times10^{-2}$°, output voltage $V_{peak} = 1.11$ V.

Uncertainty components	**Description**	**Standard uncertainty *u***	**Probability distribution**	**Sensitivity coefficient c**	**Contributed amount $c\cdot u_r$ in %**	**Degree of freedom**
$u_r(f)$	relative uncertainty of frequency readings	1.50×10^{-12}	uniform	2	1.50×10^{-10}	∞
$u_{r,S}(R_M, I_M)$	relative std. uncertainty of the magnitude of the complex sensitivity	2.06×10^{-4}	normal	1	2.06×10^{-2}	480
$u_r(\Phi)$	relative std. uncertainty of the magnitude of the angular displacement	1.33×10^{-4}	-	1	1.33×10^{-4}	
$u_{r,MA}$	prism misalignment of angle	9.56×10^{-8}°	-	1	9.56×10^{-6}	-
$u_{r,AP}$	calibration uncertainty of angle prism	2.72×10^{-6}°	normal	$1/\Phi$	8.49×10^{-3}	61
$u_{r,P}$	compensation uncertainty of the digital filter (ZMI 4004)	1.00×10^{-4}	-	1	1.00×10^{-2}	-
$u(N)$	counter uncertainty of ZMI 4004	1.64 LSB	uniform	4.21E-07/Φ	2.15×10^{-3}	∞
$u_{r,BA}$	relative std. uncertainty of background angular vibration level	3.26×10^{-7}	normal	1	3.26×10^{-5}	∞
$u_r(V)$	relative std. uncertainty of the magnitude of the voltage output	6.47×10^{-5}	-	1	6.47×10^{-3}	
$u_{r,AC}$	relative std. uncertainty of AC/DC calibration source	54 ppm	normal	1	5.4×10^{-3}	∞
$u_{r,GC}$	relative std. uncertainty of compensated gain of AD converter	1.16×10^{-5} V_{peak}	normal	$1/V$	1.05×10^{-3}	42
$u_{r,QE}$	relative std. uncertainty of quantization resolution of AD converter	8.81×10^{-6}	uniform	1	8.81×10^{-4}	∞

$u_{r,CA}$	relative std. uncertainty of the gain of calibrated charge amplifier	3.27×10^{-5}	normal	1	3.27×10^{-3}	10
$u_{r,CN}$	relative std. uncertainty of charge amplifier background noise	4.85×10^{-6}	normal	1	4.85×10^{-4}	50
$u_r(S_{RE})$	relative std. uncertainty of the magnitude repeatability of complex sensitivity	5.00×10^{-4}	normal	1	5.00×10^{-2}	
$u_{r,c}(S)$	combined uncertainty	5.60×10^{-3}	-	1	5.60×10^{-3}	
$U_r(S)$	expanded uncertainty (k = 2, L.C. = 95 %)	1.12×10^{-3}	-	1	0.112	

Table B-4: Uncertainty budget of the phase of the complex charge sensitivity at the calibration frequency of 80 Hz:
acceleration angle $\Phi_{peak} = 3.207\times10^{-2}$°, output voltage $V_{peak} = 1.11$ V.

Uncertainty components	Description	Standard uncertainty u	Probability distribution	Sensitivity coefficient c	Contributed amount $c\cdot u_r$ in °	Degree of freedom
$u_{\Delta\varphi}(R_M, I_M)$	standard uncertainty of the phase shift of the complex sensitivity	6.37×10^{-4}°	normal	1	6.37×10^{-4}	480
$\Delta\varphi(\Phi)$	standard uncertainty of the phase shift of the angular displacement	7.64×10^{-3}°	uniform	1	7.64×10^{-3}°	
$c_{AU}*u_r(\Phi)$	effect of the relative std. uncertainty of the magnitude of the angular displacement measurement	1.33×10^{-4}	-	$180/\pi$	7.62×10^{-3}	∞
$u_{\Delta\varphi,ZMI}$	effective time delay of optic receiver of ZMI 4004 board	2.02×10^{-8} s	uniform	$360\,f$	5.82×10^{-4}	∞
$\Delta\varphi(V)$	relative uncertainty of the phase shift of the voltage output	3.80×10^{-3}°	normal	1	3.80×10^{-3}	
$c_{AU}*u_r(V)$	effect of the relative std. uncertainty of the magnitude of the voltage output measurement	6.47×10^{-5}	normal	$180/\pi$	3.71×10^{-3}	∞
$u_{\Delta\varphi,CA}$	Standard uncertainty of the phase shift of the calibrated charge amplifier	8.28×10^{-4}°	normal	1	8.28×10^{-4}	50
$u_r(S_{RE})$	relative std. uncertainty of the phase repeatability of the complex sensitivity	6.78×10^{-3}°	normal	1	6.78×10^{-3}	
$u_{r,c}(S)$	combined uncertainty	1.09×10^{-2}°	-	1	1.09×10^{-2}	
$U_r(S)$	expanded uncertainty (k = 2, L.C. = 95 %)	0.022°	-	1	0.022	